Temperature-dominated spatiotemporal variability in snow phenology ~~factors~~ on the Tibetan Plateau from 2002 to ~~2021~~2022

Jiahui Xu[1,2,3], Yao Tang[1,2,3], Linxin Dong[1,2,3], Shujie Wang[4], Bailang Yu[1,2,3], Jianping Wu[1,2,3], Zhaojun Zheng[5], Yan Huang[1,2,3,*]

[1]Key Laboratory of Geographic Information Science, Ministry of Education, East China Normal University, Shanghai, 200241, China
[2]School of Geographic Sciences, East China Normal University, Shanghai, 200241, China
[3]Key Laboratory of Spatial-temporal Big Data Analysis and Application of Natural Resources in Megacities, Ministry of Natural Resources, Shanghai, 200241, China
[4]Department of Geography, Earth and Environmental Systems Institute, Pennsylvania State University, University Park, PA, 16802, USA
[5]National Satellite Meteorological Center, Beijing, 100081, China

Correspondence to: Yan Huang (yhuang@geo.ecnu.edu.cn)

Abstract. A detailed understanding of snow cover and its possible feedback on climate change on the Tibetan Plateau (TP) is of great importance. However, spatiotemporal variability in snow phenology (SP) and its influencing factors on the TP remain unclear. Based on the daily gap-free snow cover product (HMRFS-TP) with 500 m resolution, this study investigated the spatiotemporal ~~variation~~variability in snow cover days (SCD), snow onset date (SOD), and snow end date (SED) ~~in~~on the TP from 2002~~–2021~~ to 2022. A Structural Equation Model was used~~ to select the factors affecting SP as well as~~ to quantify the direct and indirect effects of meteorological factors, geographical location, topography, and vegetation greenness~~, and atmospheric pollution factors~~ on SP. The results ~~indicated~~indicate that the spatial distribution of SP on the TP was extremely uneven and exhibited~~ notable~~ temporal heterogeneity. SP showed vertical zonality influenced by elevation (longer SCD, earlier SOD, and later SED at higher elevations). ~~Meanwhile, their interannual variations tended to decrease, delay, and delay slightly from 2002 to 2021. In particular, the interannual variation in SP also had an elevation-dependent pattern below 5800 m. Meteorological factors had direct and indirect effects, vegetation greenness only had a direct impact, and geographical location, topography, and atmospheric pollution only indirectly affected SP. Undoubtedly, meteorological factors were the dominant factors in particular temperature. However, the influence of other factors cannot be ignored. As two important factors, the relative importance of temperature versus precipitation to SP shifted across elevation.~~4.62% of the TP area had a significant decrease in SCD, at a rate of −1.74 days/year. The SOD of 2.34% of the TP area showed a significant delayed trend, at a rate of 2.90 days/year; while the SED of 1.52% of the TP area had a significant advanced trend, at a rate of at −2.49 days/year. We also found a strong elevation dependence for the trend in SCD ($R = -0.73$). Air temperature, precipitation, wind speed, and shortwave radiation can directly affect SP as well as indirectly affect it by influencing the growth of vegetation, whereas the direct effect was much greater than the indirect effect. Geographical location (latitude and longitude) and topographic conditions (elevation and slope) indirectly affected SP by modulating meteorological conditions and the growth of vegetation.

Vegetation primarily influences SP by intercepting the snow and regulating the balance of the solar radiation budget. Regarding the total effect, air temperature was found to be the dominant factor. This study contributes to the understanding of snow variation in response to global warming over the past two decades by providing a basis for predicting future environmental and climate changes and their impacts on the TP.

1 Introduction

Rapid accumulation and melting of snow make it one of the most active natural materials on the Earth's surface (Gutzler and Rosen, 1992; Ma et al., 2023). The Tibetan Plateau (TP) is one of the most sensitive regions to climate change because of its unstable alpine ecosystems and fragile natural environment (Huang et al., 2017). In the past 50 years, temperature has risen at a rate of about 0.37 °C per decade on the TP (You et al., 2021). Rising temperatures inevitably affect snow accumulation and melting processes, exemplified by variations in snow phenology (SP), including snow cover days (SCD), snow onset date (SOD), and snow end date (SED) (Chen et al., 2015; ~~Guo et al., 2022~~ Ma et al., 2020). Variations in SP can in turn affect terrestrial ecosystems and feedback on regional climate (Cherkauer and Sinha, 2008). Early snowmelt also causes substantial variability in the onset date and amount of snowmelt runoff, increasing the incidence of disasters (e.g., floods) (Fyfe et al., 2017). A detailed understanding of the variability in SP and its possible feedback on climate change is of great significance to the hydrological cycle (Kraaijenbrink et al., 2021), ecological balance (Keyser et al., 2022), and societal security (Wang et al., 2017) ~~in~~on the TP.

There are typical interannual variations in the SP on the TP. Ground-measured measurements and remote sensing data have been extensively used in recent decades to better understand these changes (Ma et al., 2022; Notarnicola, 2020). Remote sensing is beneficial in high-elevation area where few ground-measured measurements are obtainable (Huang et al., 2022a). Passive microwave satellite (e.g., SMMR, SSM/I, and AMSE-R) and multispectral satellite (e.g., Landsat, Sentinel-2, and MODIS) data are widely used to retrieve snow information and reveal its variability (Chen et al., 2018). Although passive microwave data is available over an extended period, the spatial resolution (~10−25 km) is relatively coarse (Huang et al., 2017). Landsat and Sentinel-2 have a high spatial resolution (~10−30 m) but a relatively coarse temporal resolution (10 or 16 days), inadequate for monitoring temporal variability in SP (Huang et al., 2022a). Currently, the most widely available snow data used for the TP is the daily MODIS snow product (Hall et al., 1995), which has revealed that the SP on the TP has ~~changed considerably~~undergone changes in the last two decades (Ma et al., 2023; Tang et al., 2022; Wang et al., 2017). In addition, owing to the complex topography of the TP, elevation may have a particular impact on SP. However, it is still unclear whether ~~interannual variations~~trends in SP are elevation-dependent (Ma et al., 2023; Wang et al., 2021). Moreover, since the original daily MODIS images exist data gaps due to cloud cover and relatively low estimation accuracy due to complex topography of the TP (Huang et al., 2022b), most previous studies used relatively simple methods to fill data gaps and did not consider topographic effects. Using snow products without topographic corrections may result in inaccurate ~~SP~~ extraction of SP, further affecting the analysis result of interannual variations. Huang et al. (2022b) generated a daily gap-free snow product on the TP by employing a Hidden Markov Random Field (HMRF) framework to MODIS product (HMRFS-TP). The data gaps were filled by optimally integrating spatiotemporal, spectral, and environmental information. Accuracy of HMRFS-TP was significantly improved over the complex topography, providing spatiotemporally continuous information on snow distribution over an extended period with high accuracy.

Regarding the influencing factors on SP of the TP, previous studies have highlighted a complex and heterogeneous situation in which SP is driven by meteorological factors, topographic conditions, geographical location, and vegetation greenness (Pulliainen et al., 2020; Qi et al., 2021; You et al., 2020). ~~Temperature~~The impact of air temperature and precipitation ~~are the two dominant meteorological factors affecting SP~~on snow cover has been extensively studied (Li et al., 2022; Tarca et al., 2022). ~~Temperature defines precipitation-to-snowfall ratio and snowpack melt (Ishida et al., 2019).~~However, SP is also closely associated with other meteorological factors, such as wind and humidity~~; however,~~. But their quantitative influence on SP on the TP has not been discussed further (~~Ishida et al., 2019;~~ Ma et al., 2022; Xie et al., 2017). Topographic characteristics (Guo et al., 2022) and vegetation greenness (Qi et al., 2021) are also considered responsible for SP. Elevation is an essential factor that influences SP because snow accumulates more at higher elevations. Steeper slopes may receive less snow than flatter ones due to gravitational pull (Li et al., 2011). Vegetation greenness changes the snow redistribution process by intercepting snow, and affects spatial pattern and melt rate of surface snow by regulating the solar radiation budget balance (Barrere et al., 2018).~~ Recent studies (Kang et al., 2019) have found that the deposition of atmospheric pollution (e.g., black carbon) can influence snowfall as well as snowmelt, and thus should be regarded as an essential physical factor affecting snow variation on the TP. For instance, increased black carbon and dust reduced the SCD by 3–4 days on the TP (Zhang et al., 2018).~~

Although much research has examined the variability in the SP and its influencing factors on the TP, uncertainties and limitations remain. Previous studies have mainly focused on the response of SP to temperature and precipitation, but few studies have quantitatively explored other associated factors influencing SP. Additionally, many analyses have primarily focused on examining the relationship between SP and individual influencing factors, without taking into account the interrelationships among these factors. Associated factors may have both direct and indirect impacts on SP. For example, temperature can affect SP directly, as well as indirectly by influencing the growth of vegetation (Qi et al., 2021). The specific process by which each factor influences SP (i.e., directly, or indirectly) has not been elucidated. The Structural Equation Model (SEM) is a suitable method for studying such coupling relationship, which can quantitatively explain the direct and indirect relationships between factors (Grace et al., 2010; Shen et al., 2022; Zhang et al., 2022). Here we adopt this approach to explore the mediating effects between SP and associated factors.

In this study, we conducted a comprehensive investigation on the spatiotemporal variability in SP on the TP over the past two decades (2002–~~2021~~2022), based on the daily gap-free HMRFS-TP dataset, and further quantified the influence of associated factors on SP. The main goals are to (1) calculate SP parameters (SCD, SOD, and SED), and analyze their spatiotemporal variability; (2) examine whether ~~interannual variation~~the trends in SP ~~on the TP is~~are elevation-dependent; and (3) ~~reveal~~quantify the direct and indirect effects of associated factors on SP.

2 Study area and data

2.1 Study area

The TP (26°00′12″N-39°46′50″N, 73°18′52″E-104°46′59″E~~) has an average elevation of over 4000 m and an area of approximately 2.5 × 10^6 km^2 (Figure 1). Under the background of global warming, enormous changes have taken place in the TP cryosphere.~~, Figure 1) is the largest snow cover area in the middle latitudes of the Northern Hemisphere, with 10^5 km^2 of glaciers and an annual snowfall of 41.9 × 10^9 m^3 (Yao et al., 2012). The southeastern TP is warm and moist while the northwestern TP is cold and dry. The average annual temperature ranges from −6 to 20 °C and the average annual precipitation ranges from 150 to 800 mm (Wang et al., 2023). Temperature in its permafrost region is rising at about three times the speed of global warming (Wang et al., 2022). As a topographic barrier, the TP forces air mass up and produces cooling effects (Wu et al., 2015), further influences the thermodynamic properties of atmospheric circulation, strength and duration of Asian monsoon systems, global climate, and energy budge (Fan et al., 2019). ~~The southeast is warm and moist while the northwest is cold and dry in the TP (Wang et al., 2023).~~ It is the source of several prominent Asian rivers (e.g., the Yellow River, Yangtze, Indus, and Mekong), which are primarily fed and regulated by meltwater from glaciers and snow (Chen et al., 2022). ~~Snowmelt water is used for livelihoods and irrigation in the region and its surrounding areas. The change in SP affects the vegetation greenness of the plateau and its surrounding areas.~~

2.2 Datasets

2.2.1 Snow cover product

The daily gap-free HMRFS-TP at 500 m resolution from 2002 to ~~2021~~2022 was used to extract SP (Huang et al., 2022b). The HMRF technique produces a dataset (Huang et al., 2018) that optimally couples spatiotemporal, spectral, and environmental information to fill data gaps in original MODIS images. Accuracy of the HMRFS-TP is 91.36% and 98.29% based on snow maps derived from Landsat images and *in situ* observations, respectively. The estimation accuracy is notably improved in snow transitional periods and complex topography with higher elevations and sunny conditions. To determine the SP (including SCD, SOD, and SED), we specify the snow season from 1 September of the ~~last~~previous year to 31 August of the current year (Tang et al., 2022). The snow accumulation season is defined as from 1 September of the previous year to February 28 (or 29) of the current year, and the snowmelt season is from 1 March to 31 August of the current year (Ma et al., 2023). The SP for ~~19~~20 snow seasons from 1 September 2002 to ~~31August 2021~~31 August 2022 was extracted based on the long-term HMRFS-TP dataset.

2.2.2 Meteorological data

~~To explore the influence~~We used daily meteorological dataset at 1/30° resolution from 2002 to 2022 to investigate the impact of meteorological factors on SP, ~~monthly~~including air temperature~~ and~~, precipitation ~~from 2002to 2021 with 1 km resolution were used (Peng et al., 2019). This dataset was generated from two global high-resolution climate data through a delta spatial~~

~~downscaling model. Monthly~~, specific humidity, wind speed, and downward shortwave radiation ~~with 0.1° resolution from 2002 to 2018 were created~~ . This dataset was generated by ~~coupling~~integrating *in situ* observations, remote sensing, and reanalysis dataset (He et al., 2020~~).~~; Yang et al., 2023). All ~~monthly~~daily meteorological data were ~~averaged for each snow season and~~ resampled to 500 m to maintain consistency with the MODIS snow product. We calculated average air temperature, average humidity, average wind speed, total precipitation, and total shortwave radiation for each snow season, snow accumulation season, and snowmelt season to examine their relationship with SCD, SOD, and SED, respectively (Chen et al., 2018; Ma et al., 2023).

2.2.3 Digital Elevation Model (DEM)

The 30 m DEM data, available from the USGS Earth Explorer (https://earthexplorer.usgs.gov), was resampled to 500 m resolution. Topographical parameters including elevation, slope, and aspect were calculated from it.

2.2.4 Land surface reflectance product

Compared with other vegetation indexes, the Normalized Difference Greenness Index (NDGI) (Yang et al., 2019) has been proven to more accurately represent the vegetation greenness growth status in snow-covered areas such as the TP (Xu et al., 2022a; Xu et al., 2022b). Here, we calculated the NDGI based on MODIS Terra surface reflectance MOD09A1 with 500 m resolution and an 8-day repeat cycle from 2002 to ~~2021~~2022 (Vermote, 2021). The bands 4, 1, 2 of MOD09A1 were used to calculate the NDGI. The maximum complex method was implemented to filter noise and fill data gaps owing to cloud and atmosphere in NDGI series (Xu et al., 2022b). The ~~annual~~ average NDGI ~~time-series composite data~~was calculated for each snow season ~~were obtained~~, snow accumulation season, and snowmelt season.

~~2.2.5 **Atmospheric pollution data**~~

~~We used two essential atmospheric pollution datasets, Black Carbon (BC) emissions (g km^{-2}) and Aerosol Optical Depth (AOD) concentration (μg m^{-3}), to explore the interaction between atmospheric pollution and SP. The monthly global BC emission estimates covered 73 detailed sources at a 0.1° resolution from 2002 to 2017 (Xu et al., 2021). The monthly AOD dataset at a resolution of 1 km was obtained by synergistically integrating multimodal aerosol data (Bai et al., 2022). We converted all monthly BC emissions and AOD concentration data to the annual average during the snow season and resampled them to 500 m resolution.~~

~~2.2.6~~ 2.2.5 Auxiliary data

Snow depth recorded from meteorological stations was used as the reference value (ground-observed SP) to validate the accuracy of the satellite-derived SP parameters. Due to instrument machine failure or man-made errors, not all meteorological stations (approximately 137) on the TP recorded snow depth values every day. This resulted in many data gaps during the snow season, which were not sufficiently continuous to extract ground-observed SP. Therefore, 24 meteorological stations with daily records were selected for validation (Figure 1).

3 Methods

~~-~~Figure 2 illustrates the workflow of this study. The SP parameters (SCD, SOD, and SED) were first extracted from the daily HMRFS-TP dataset, and their spatiotemporal ~~variations~~variability were analyzed. We then adopted SEM to ~~identify~~quantify the ~~factors that were relatively important to SP: meteorological factors, topographic conditions, geographical location, vegetation greenness, and atmospheric pollution. The~~ direct~~/~~ and indirect effects of ~~these~~associated factors on SP~~ were also analyzed using SEM. We~~. The impact of relatively important factors on SP was discussed in further ~~quantitatively discuss the effects of these factors on SP~~depth.

3.1 Snow phenology extraction and accuracy assessment

Three parameters, SCD, SOD, and SED, were derived to describe SP in each snow season and were calculated from the daily HMRFS-TP dataset at the pixel level. SCD is the sum of days when a pixel is covered by snow across the snow season. SOD is the first date when a pixel is covered with snow stay at least 5 days in a snow season. SED is the last date on which a pixel was identified as snow for 5 consecutive days (Tang et al., 2022). Using a threshold value of 5 days can reduce the influence of frequent short-term variability (e.g., snowmelt and accumulation in early spring and late autumn), which has been a widely used threshold on the extraction of SOD and SED (Guo et al., 2022; Wang et al., 2017; Xu et al., 2022b). Calculations of SP were excluded from regions containing lakes.

The accuracy of the extracted SP was validated using ground-observed SP from snow depth measured by meteorological stations. The ground-observed SP was calculated as follows. First, all recorded snow depth values were reclassified as snow or no snow based on a 3 cm threshold (Huang et al., 2022a; Huang et al., 2022b). For each snow season, meteorological stations that recorded more than 200 days of snow depth were selected (Hao et al., 2022; Zhao et al., 2022). Days without snow depth records at the selected stations were supplemented with remote sensing images (Landsat series, Sentinel-2, etc.) of these days. ~~Finally, stations~~Stations with fewer than 20 snow-covered days and fewer than 5 consecutive snow-covered days during the snow season were excluded. ~~Fifty-six~~After applying these criteria, a total of 56 ground-observed SP from 24 ~~meteorological~~ stations were ~~collected~~used for accuracy ~~assessment~~validation.

3.2 Trend analysis

To explore the interannual variation trend and trend significance in SP from 2002 to ~~2021~~2022, the Theil-Sen non-parametric regression (Sen, 1968) and Mann-Kendall (M-K) tests (Hirsch et al., 1982) were applied to each pixel. The Theil-Sen method has the advantage of dealing with non-normally distributed data, and is robust against outliers compared with traditional linear regression (Theil, 1992).

$$\beta = Median\left(\frac{x_j - x_i}{j-i}\right),\ 1 < i < j < n, \tag{1}$$

where β is the trend slope; a positive value denotes the trend of SP as a delay/extension, and a negative value assumes SP is advanced/delayed. n =19, x_i is the i^{th} value in 19 years. Same as x_j and j^{th}.

The M-K test is a non-parametric approach for monotonic trend that has been used for trend detection of hydrological and meteorological time series (Qi et al., 2021). The Z value assumes the temporal trend is statistically significant:

$$Z = \begin{cases} \frac{S-1}{\sqrt{Var(S)}}, if\ S > 0 \\ 0, if\ S = 0 \\ \frac{S+1}{\sqrt{Var(S)}}, if\ S < 0 \end{cases}, Var(S) = \frac{n(n-1)(2n+5)}{18}, \tag{2}$$

$$S = \sum_{i=1}^{n-1} \sum_{j=i+1}^{n} \begin{cases} 1, if x_j > x_i \\ 0, if\ x_j = x_i, 1 < i < j < n, \\ -1, if\ x_j < x_i \end{cases} \tag{3}$$

when $|Z|>$1.28, 1.64, and 2.32, the tests were significant at levels of 0.1, 0.05, and 0.01, respectively.

Since snow cover may not be present each year, to evade unnatural results caused by a small amount of data, only the pixels with at least recorded 6 years for the SP were used for the interannual trend evaluation (Xu et al., 2022b).

3.3 Structural equation model

We used SEM to ~~identify relatively important factors and~~ quantify ~~their~~the direct and indirect effects of various factors on SP. It is a multivariate collection of methods that can simulate the interaction between various factors at the same time, supplying a framework for extrapolating cause-effect relationship and revealing direct and indirect relations between independent and dependent variables (Grace et al., 2010). SEM includes Covariance Based-Structural Equation Model (CB-SEM) and the Partial Least Square Structural Equation Model (PLS-SEM) (Venturini and Mehmetoglu, 2019). Contrasted with CB-SEM, PLS-SEM focuses on mining sample information and can reflect the nature and structural characteristics of objects as much as possible, making it more suitable for exploring newly constructed structural models (Hair et al., 2011; Ringle et al., 2012). More importantly, PLS-SEM is a nonparametric model that does not require a normal distribution of samples and has considerable potential for remote sensing applications (Lopatin et al., 2019; Zhang et al., 2022). Therefore, we ~~selected~~adopted PLS-SEM ~~to test relatively important factors and their direct and indirect effects on SP~~for further exploration.

When using PLS-SEM with normalized factors, multicollinearity diagnosis, and model fit evaluation are essential for model quality evaluation. Multicollinearity diagnosis (Cenfetelli and Bassellier, 2009), which relies mainly on VIF ~~and tolerance~~, is an important issue in model quality evaluation ~~owing~~. High multicollinearity between factors may cause inaccurate path coefficient, leading to ~~its valuable for unstable factor weights.~~ these factors being misinterpreted as unimportant or invalid (Hair et al., 2010). The model fit evaluation uses approximate fit indices like SRMR (Standardized Root Mean Square Residual) and NFI (Normed Fit Index). A desirable PLS-SEM is characterized by SRMR less than 0.08 and NFI greater than 0.90. To interpret the SEM results, a standardized path coefficient implies the direct effect of one factor on another, and its significance ($p < 0.05$) can be evaluated by ~~d-~~resampling procedures (Hair et al., 2011). The path coefficient was solved iteratively using ordinary least squares, and the significance ($p < 0.05$) of each path coefficient was obtained by bootstrapping (5000 iterations). The indirect effect of one factor on another can be calculated through multiplying all indirect path coefficients, and the total effect is the sum of the indirect and direct effects.

4 Results

4.1 Accuracy assessment of the extracted snow phenology

Figure 3 shows the accuracy of the satellite-derived SP parameters ~~during 2002–2021,~~ compared ~~against~~with the ground-observed SP. The satellite-derived SCD, SOD, and SED values were in line with ground-observed ones, with *R* of 0.77, 0.95, and 0.97 ($p < 0.01$), respectively. The bias of ground-observed and satellite-derived SCD, SOD, and SED were −1.75, −2.39, and 3.43 days, indicating that the satellite-derived SCD was less than the actual SCD, and the satellite-derived SOD was earlier than the actual SOD. In contrast, satellite-derived SED occurred later than the actual SED. Relevant studies have shown the bias of satellite-derived SP parameters ranges from 0 to 10 days (Chen et al., 2018; Hao et al., 2022; Wang et al., 2021). The biases (−2.39, 3.43, and −1.75 days) in our study were within this range.

4.2 Spatial patterns and temporal trends of snow phenology

The spatial patterns and temporal trends of SP at the pixel level are shown in Figures 4 and 5, respectively. Figure 4a indicates the spatial distribution of the multiyear averaged SCD from 2002 to ~~2021~~2022, showing a highly uneven snow cover distribution across the plateau. Areas with an SCD of more than 60 days are considered as stable snow cover areas and sources of water (Tang et al., 2022), accounting for approximately 17.~~69~~07% of the total TP and primarily distributed in high-elevation mountain ranges. Some high-elevation areas had an SCD exceeding 180 days, accounting for approximately 7.~~55~~40% of the entire TP, distributed primarily in the western Kunlun, Himalaya, and Nyainqentanglha mountains. Areas of low SCD (< 20 days) accounted for ~~56.69~~55.95% of the total TP, mainly concentrated in low-elevation areas and the hinterland of the plateau. Overall, the pattern of SCD was in line with topography in visual sense, displaying the regularity of a high SCD in high-elevation mountains and low SCD in the low-elevation plains. We also examined the ~~interannual trends of the~~ temporal trend in SCD and ~~their~~its significance. As Figure 5a shows, the SCD decreased in ~~64.18~~50.59% of the TP during the ~~19~~20-year period, and significantly decreased by 4.~~29~~62% of the ~~entire area~~total TP at a mean rate of −~~2.09~~1.74 days/year ($p < 0.1$), primarily in the west Kunlun, east-central Himalaya, and south Nyainqentanglha mountains. In contrast, areas with significantly increased SCD accounted for ~~35.82~~2.45% of the total TP~~, increased significantly by 1.84%~~ at a mean rate of ~~the entire area~~1.12 days/year ($p < 0.1$), and was mainly scattered in the east-central part of the TP.

Distribution of SOD and SED~~ distributions~~ over the TP also presented extreme spatial heterogeneity, which was visually consistent with elevation (Figures 4b and 4c). DOS (day of the snow season) 1 is equivalent to September 1 of the previous year. SOD was mainly concentrated in DOS 90–180 (December–February), whereas SED was concentrated primarily in DOS 150–240 (February–April~~), indicating snow on the TP mostly disappeared at the end of April.~~). In high-elevation mountain ranges, SOD appears earlier in general, whereas SED shows later. But in low-elevation areas such as the hinterland of the TP, SOD starts later and SED appears earlier. Not only are the variations in SOD and SED spatially complicated, but they also exhibited significant temporal heterogeneity (Figures 5b and 5c). ~~Areas with~~58.56% of the total TP had delayed SOD ~~accounted for 56.86~~, and 2.34% of the TP~~, with the delay~~ had a statistically significant ~~in approximately 3.35% of the total area,~~ ($p < 0.1$) delayed SOD at a mean rate of ~~3.64~~2.90 days/year (~~$p < 0.1$) (~~Figure 5b). In contrast, ~~the area~~areas with significantly advanced SOD only accounted for ~~approximately~~ 0.~~6~~46% of the total area at a mean rate of −3.69 days/year ($p < 0.1$), and was sparsely distributed in the north~~-~~western and eastern TP~~ at a mean rate of −3.3 days/year. Consistent with SOD,~~. For SED~~ exhibited a delayed~~, 98.41% of the TP showed no significant trend~~ across most of the TP. One difference was SED delayed faster over large area in the hinterland of the TP (Figure 5c). Areas with significantly~~, 1.52% showed a significant advanced ~~and delayed SED accounted for only 1.35% and 2.07% of the TP, respectively~~trend at a rate of −2.49 days/year ($p < 0.1$), and 0.07% showed a significant delayed trend ($p < 0.1$) (Figure 5c).

4.3 Direct and indirect effects of important factors on snow phenology

Based on the related literature (Guo et al., 2022; Huang et al., 2020; ~~Kang et al., 2019;~~ Qi et al., 2021), ~~13~~11 initial associated factors in ~~five~~four categories were selected: meteorological factors (air temperature, precipitation, wind speed,~~ specific~~ humidity, and shortwave radiation), geographical location (latitude and longitude), topography (elevation, slope, and aspect), and vegetation greenness (NDGI~~), and atmospheric pollution (BC and AOD). Because~~). First, multicollinearity diagnosis was performed on all initial factors, among which humidity did not pass the ~~construction of~~ multicollinearity diagnosis (VIF=10.8) and was excluded. Then, we constructed a SEM ~~requires prior knowledge,~~using the remaining factors and established multiple paths in ~~SEM based on the above 13 factors were investigated, and non~~the model. Non-significant and low~~-~~ coefficient paths ~~should be eliminated theoretically. In this step, the path coefficients of AOD were non-significant for each factor or even for all SP. Therefore, we eliminated AOD~~were removed, and ~~calculated~~ the total effect ~~of the remaining factors on SP~~(TE) of each factor was calculated based on the final paths (Figure 6). Factors with a small absolute ~~total effect were~~TE should be removed because of their low contribution and limited explanations~~ of SP~~. An appropriate threshold was selected as the basis for factor elimination. Hair et al. (2011) indicated that there is no uniform standard for selecting thresholds in different research fields. Considering the rationality of factor selection and referring to relevant literature (Shen et al., 2022; Zhang et al., 2022), we used 0.01 as the threshold for factor elimination. Aspect was eliminated for ~~SCD and SED, and aspect and wind speed was eliminated for SOD~~all SP (Figure 6~~). The~~), and the final ~~SEM models~~SEMs were constructed to discuss the direct and indirect effects of the remaining 9 factors.

~~The~~Figure 7 presents the results of the final SEM and its standardized regression path coefficient (PC) ($p < 0.05$~~)~~). It indicates that there are ~~shown in Figure 7. Complex~~complex interactions ~~exist~~ between SP and ~~different~~associated factors on the TP. Temperature, wind speed, NDGI, and shortwave radiation had negative effects on SCD and positive effects on SOD, while the other factors had positive effects on SCD and negative effects on SOD. Furthermore, temperature, wind speed, and shortwave radiation had negative effects on SED, while the remaining factors had positive effects on SED. Meteorological factors ~~had~~(air temperature, precipitation, wind speed, and shortwave radiation) exerted both direct and indirect effects on SP, whereas vegetation greenness ~~only~~ (NDGI) mainly had a direct impact, and geographical location~~,~~ (latitude and longitude) and topography~~,~~ (elevation and ~~atmospheric pollution only~~slope) had an indirect effect on SP (Figure 7). Meteorological factors were the dominant factors affecting SP, especially the temperature, which had the strongest effect on SCD, SOD, and SED, with ~~a total effect (~~the TE~~)~~ value of −0.~~708~~447, 0.~~371~~272, and −0.~~562~~379, respectively. The influences of precipitation ~~and specific humidity~~ on SCD and ~~SED~~SOD were also relatively significant (~~TC~~ absolute value of TE > 0.~~16).~~19). However, ~~their influence~~its impact on ~~SOD activity~~SED was limited (TE=0.049). Wind speed exhibited a strong effect on SCD and SED (absolute ~~TE~~ value ~~<~~of TE > 0.~~1). The~~15), while its effect on SOD was relatively limited (TE=0.062). The effect of ~~vegetation greenness~~NDGI on SCD and SOD was strongest (~~PC = −0.126) (Figure 7a), whereas it had little effect on SOD and SED (absolute values of PC < 0.04) (Figures 7b and 7c).~~absolute value of TE > 0.17). Geographical location and topographic conditions affected SP by determining meteorological conditions and the ~~distribution~~growth of ~~climate and~~ vegetation ~~greenness~~. For example, elevation indirectly affected SCD by assessing the distribution of temperature (PC = −0.~~990~~805), precipitation (PC = −0.261), shortwave radiation (PC = 0.330), wind speed (PC = ~~−~~0.~~301~~418), and ~~specific humidity~~NDGI (PC = −0.~~554~~649); hence, the ~~TC at elevation on the SCD was 0.510 (Figure 7a). Therefore, the influence~~ TE of elevation on ~~SP cannot be ignored and is second only to that of temperature (Figure 7). Slope mainly affected SP by influencing the distribution of precipitation and temperature. Its influence on SCD was the largest (TE = 0.188), followed by SED (TE = 0.147), and SOD (TE = −0.08). The PC~~ the SCD was 0.290 (Figure 7a). The influence of ~~longitudinal and shortwave radiation was relatively large (PC = 0.882). The influence of longitude~~latitude on all ~~the~~ SP parameters was greater than that of ~~latitude. Although the TE of the BC was not particularly large (TE > 0.02), its influence cannot be ignored.~~

~~In summary, temperature was the dominant factor affecting all SP parameters on the TP, followed by elevation. Temperature, NDGI, wind speed, and shortwave radiation negatively affected SCD and SED, whereas other factors positively affected SCD and SED. Temperature and NDGI positively affected SOD, whereas the other factors negatively affected SOD~~longitude.

5 Discussion

Compared to traditional statistical methods, the SEM adopted in this study can ~~reveal~~accurately quantify the direct and indirect relationships between SP and associated factors~~, which is suitable~~. This makes it particularly well-suited for understanding ~~their~~the mediating effects of these factors. Based on the results of this model, the influences of relatively important factors are discussed below.

5.1 Response of snow phenology to meteorological factors

Meteorological factors ~~had both direct~~(air temperature, precipitation, wind speed, and ~~indirect effects on~~shortwave radiation) can directly affect SP~~, but~~ as well as indirectly affect it by influencing the growth of vegetation, whereas the direct effect was much greater than the indirect effect. ~~Temperature~~Among these factors, air temperature was the dominant meteorological factor~~, followed by precipitation~~. A temperature below 0 ℃ is conducive to the increase and maintenance of snow cover, resulting in longer SCD, earlier SOD, and later SED (Moran-Tejeda et al., 2013; Scalzitti et al., 2016). ~~Non-negligible effect of temperature on SP has been demonstrated previously (Tang et al., 2022). However, previous studies have shown that precipitation has a low~~As another important factor, precipitation has been indicated by prior research to have a comparatively lower contribution to SP (Guo et al., 2022; Huang et al., 2020; Wang et al., 2021), which is inconsistent with the results of our research~~.~~ (Figure 7). This discrepancy may be caused by the different resolutions of precipitation data. The spatial resolution of the precipitation data we used was ~~1~~approximately 3 km, while the resolution in previous studies was relatively rough (25 km or data from meteorological stations). The ~~1~~3 km resolution precipitation data we used reveals greater details of precipitation distribution and provides more accurate precipitation information, thus obtaining a more reliable correlation between precipitation and SP.

To further explore the response mechanisms of SP to temperature and precipitation, their relationship was analyzed at the pixel level using Pearson's correlation coefficients (Figures 8). SCD and SED exhibited a negative correlation with temperature across the majority of regions, accounting for 88.09% and 73.81% of the TP, respectively (Figures 8a and 8e). Conversely, they demonstrated a positive correlation with precipitation in 59.67% and 61.02% areas of the TP (Figures 8b and 8f). SOD was positively correlated with temperature in 78.02% of the TP (Figure 8c), and displayed a negative correlation with precipitation in 70.90% of the TP (Figure 8d). We also calculated the correlation coefficients of SP with temperature and precipitation for each elevation ranges (Figures 8g, 8h, and 8i). The role of temperature and precipitation in SP varies with elevation. In areas with low elevation (< 1500 m) and high elevation (> 6700 m), the relationships between SP and temperature and precipitation were complex, with neither factor dominating significantly. For SCD, the influence of precipitation exceeded that of temperature and became more important in 1500–5400 m (Figure 8g). However, temperature played a more crucial role in 5400–6700 m. Similarly, the effect of precipitation on SED was more significant in 1800–5400 m, after which the effect of temperature was more important in 5400–6700 m. The correlation between SOD and precipitation was stronger than its correlation with temperature across 4700–5500 m. Overall, we identified that relative importance of temperature and precipitation shifts with elevation. Our findings differ from previous studies, where researchers generally found an elevation threshold where the importance of each changed. For instance, Moran-Tejeda et al. (2013) discovered a threshold elevation of approximately 1400 m, below which temperature was the primary explanatory variable of snow cover in Switzerland, and above which precipitation was a better predictor. Scalzitti et al. (2016) found a range of threshold elevations (1580 m–2181 m) that separated the importance of temperature from that of precipitation in the western United States. The reasons for such difference with our research could be as follows: (1) the complex terrain and different climate conditions of the TP, and (2) the unique changes in temperature and precipitation at different elevations on the TP. The confounding influence of warming temperatures and varying precipitation remains a challenge in explaining the observed variations in the SP.

~~To further explore the response mechanisms of SP to temperature/precipitation, their relationship was analyzed at the pixel level and at different temperature/precipitation gradients using Pearson's correlation coefficients (Figures 8 and 9). For 79.79% of the area, SCD was negatively correlated with temperature, and areas with strong negative correlations were primarily in eastern TP (Figure 8a). Between −5°C and 23°C, the negative correlation between SCD and temperature was significant (*p*<0.1) (Figure 8b). Temperature had both positive (56.63% of the TP) and negative (43.37% of the TP) correlations with SOD activity (Figure 8c). However, the correlations were not significant (*p*>0.1) for all temperature gradients (Figure 8e). Consistent with SCD, SED was negatively correlated with temperature (66.38% of the TP area) (Figure 8e). From −10°C to −4°C, the negative correlation between SED and temperature was significant (*p*<0.1). SCD and SED were mainly positively correlated with precipitation, and areas with strong positive correlation were concentrated primarily in the hinterland and southwest of the plateau (Figures 9a and 9e). In contrast, SOD was negatively correlated with precipitation in most areas (Figure 9b).~~

This study still has some limitations in exploring the effect of meteorological factors on SP. We calculated the average (or total) metrics of each meteorological factor during the snow accumulation season to explore their relationship with SOD using SEM. Similarly, we calculated the average (or total) metrics of each meteorological factor during the snowmelt season to investigate their relationship with SED (Chen et al., 2018; Ma et al., 2023). The purpose of this is to address the time dependence of meteorological factors. In the future, we intend to explore more methods for effectively separating the time dependence of meteorological factors when studying their effects on snow phenology. Additionally, previous studies suggested potential lagging effects of meteorological factors on the SP of TP. For instance, Li et al. (2019) found that anomalous precipitation could lead to subsequent snow cover variations on the TP with a delay of approximately 5 days. Ren et al. (2018) observed a strong negative correlation between snow cover and the average temperature of 1 to 4 months prior to snow accumulation. Despite the potential importance of lagging effects on the snow cover of TP, our SEM model requires concurrent observations of dependent and independence variables for accurate quantification of the causal relationships between them. Therefore, the lagging effects were neglected in this study.

5.2 Topography control on snow phenology

Previous studies have demonstrated the effect of complex topography on SP (Guo et al., 2022; Jain et al., 2008; Ma et al., 2020). Still, they did not reveal the specific action processes (direct or indirect) of various topographic factors~~.~~ affecting SP. This study ~~calculated the PC between topographic factors and SP using SEM, indicating~~indicated that topographic conditions indirectly affected SP by ~~first affecting~~ modulating meteorological ~~factors (such as temperature and precipitation).~~conditions and the growth of vegetation using SEM. Elevation is the primary factor, due to its vital effect on local microclimates, particularly in mountainous regions. In high-elevation mountains, the temperature and specific humidity are lower and snowfall is higher, creating favourable conditions for snowfall and maintenance. Owing to strong blocking effect from large mountains, most areas of the hinterland of the TP has relatively scarce snow (Wang et al., 2017). Snow is more likely to slide on a steeper slope, which prevents snow accumulation, whereas a flatter slope is conducive to snow deposition. As shown in Figure 7, slope had little effect on SOD (compared with SCD and SED), indicating that the ~~onset of~~ snow accumulation was mainly influenced by climate and less by slope.

~~Elevation had a significant effect on SP, but whether the interannual variation in SP on the TP was elevation-dependent was unknown. To investigate this uncertainty, we calculated the interannual variation in SP for each elevational gradient (Figure 10). Almost all the SP parameters showed distinct elevation-dependence: SCD decreased as elevation increased from 1200–5800 m, while SOD and SED advanced from 700–2600 m, and SOD was slightly delayed from 5400–5800 m. At elevations above 5800 m, the elevation dependence was not significant. This may be because the temperature remained below 0 °C at higher elevations, there would likely be no effect on snow cover variability. Thus, elevation dependence was not significant at high elevations. Our conclusions are consistent with those of Ma et al. (2023). In contrast, Ma et al. (2020) showed no elevation dependence of SP on the TP. However, their results were based on meteorological stations concentrated in the eastern part of the TP, with the western TP barely represented, which may have caused the disparity in findings.~~

~~The relative importance of temperature versus precipitation for SP shifts with elevation (You et al., 2020). We investigated the relationships between SP and temperature/precipitation at different elevations to further examine the effects. As shown in Figure 11, the roles of temperature and precipitation in SP varied along diverse elevation gradients. For the SCD, with an increase in elevation in the 100–3000 m range, the importance of temperature was higher than that of precipitation. However, when the elevation reached 3100 m, the impact of precipitation became more substantial and was greater than that of temperature between 3100–6100 m. Temperature was more important than precipitation at higher elevations (>6200 m). The correlation between SOD and precipitation was stronger than that with temperature between 1800–4700 m, whereas temperature was more important between 4700–6700 m. However, above 6700 m, SCD and temperature/precipitation correlations became complicated, and neither showed greater importance. Similar to SOD, precipitation had a more significant impact on SED between 1800–4000 m, and the importance of temperature and precipitation was almost equal above 6100 m. One difference was that in the 5100–6100 m range, precipitation was still more critical to SED.~~

~~Overall, we identified that neither temperature nor precipitation showed consistently higher essential as elevation increased. Our findings differ significantly~~Elevation had a significant effect on SP, but whether the trends in SP from 2002 to 2022 on the TP was elevation-dependent was unknown. To investigate the elevation effect, we divided elevation into 50 m intervals, and the average trend values of statistically significant pixels ($p < 0.1$) were calculated for each elevation category. Then, we selected elevation categories with more than 50 samples to analyze the correlation between trends in SP and elevation. Our finding reveals a strong negative correlation between trend in SCD and elevation, with a correlation coefficient of −0.73 (Figure 9a). This negative correlation was strongest in 0−4000 m and 4900−5900 m. A moderate positive correlation exists between the trend in SOD and elevation ($R = 0.59$), and this positive correlation was most significant in 4100−5800 m (Figure 9b). The correlation between SED and elevation was 0.33, which was not significant (Figure 9c). Therefore, there exists a strong elevation dependence for the trend in SCD ($R = -0.73$), a moderate elevation dependence for the trend in SOD ($R =$

0.59), and no significant elevation dependence for the trend in SED (R = 0.33) from 2002 to 2022. The elevation dependence of the SCD trend is consistent with the previous study of Ma et al. (2023). However, Ma et al. (2020) found no elevation dependence for both SOD and SED trends. This discrepancy is very likely because the meteorological data used in their study were mainly distributed in the eastern TP while the western TP was much less considered. This further highlights the high spatial heterogeneity of SP in TP.

The non-significant elevation dependence of SED is due to the competing effects of the delayed trend within 3800−4900 m elevation and the advanced trend of other elevation ranges (Figure 9c). To explain the counterintuitive delayed trend in the context of regional warming, we further applied a structural equation model to explore the causal relationships. The results indicate that wind speed significantly influences the delayed trend in SED, exhibiting a strong positive correlation with a total effect of 0.497 (Figure 9d). The delayed trend in SED becomes more pronounced as wind speed increases. This effect of wind speed on snow cover is mainly through blowing snow process, which lead to increased snow accumulation through snow redistribution and thus a delayed trend in SED regionally. Li et al. (2012) also found a distinct occurrence of blowing snow at an elevation of 4146 m, where pronounced redistribution of snow cover occurred.

~~from previous studies, where researchers generally found an elevation threshold where the importance of each changed. For instance, Moran-Tejeda et al. (2013) discovered a threshold elevation of approximately 1400 m, below which temperature was the primary explanatory variable of snow cover in Switzerland, and above which precipitation was a better predictor. Scalzitti et al. (2016) found a range of threshold elevations (1580–2181 m) that separated the importance of temperature from that of precipitation in the western United States. The reasons for such difference with our research could be as follows: (1) the higher elevation and different climate conditions of the TP, and (2) the unique changes in temperature/precipitation at different elevations on the TP, especially the greater increase in temperature and the greater decrease in precipitation at high elevations. The confounding influence of warming temperatures and varying precipitation remains a challenge in explaining the observed variations in the SP.~~

5.3 Other factors affecting snow phenology

~~Geographic location determines the total solar radiation received by the plateau. We further quantified longitudinal/latitudinal zonation of the SP, as shown~~The TP has a vast territory spanning multiple longitude and latitude zones, and longitude and latitude cannot be ignored in ~~Figure 12.~~snow cover research. A greater longitude (i.e., further east) caused a shorter SCD, later SOD, and earlier SED (Figure ~~12a~~4). From east to west, SCD decreased by 123 days, SOD was delayed by 77 days, and SED advanced by 48 days. The ~~decreased SCD and advanced SED occurred at low longitudes (73°E–82°E), whereas~~ elevation of the ~~other areas showed slightly increased SCD and decreased SED. The SOD showed a delayed trend in almost all longitudes. From low to high latitudes, SCD decreased to an inflection point at 34°–35°and then increased gradually. The SOD and SED advanced to inflection points at 29°–30° and 32°–33°, respectively, and then were steadily delayed (Figure 12b). SCD, SOD, and SED generally showed, respectively, decreasing, delayed, and delayed inter-annual variation trends with increasing latitude. Previous studies have mainly concentrated on the response of SP to latitude, whereas the role~~ TP decreases from west to east, resulting in a correlation between elevation and longitude (R = 0.532, Figure 10a). This correlation can cause the effect of longitude ~~has rarely been discussed (Guo et al., 2022; You et al., 2020). Longitude had a non-negligible effect~~ on SP folded under the effect of elevation on SP ~~in this study. Because different~~. However, controlling the influence of elevation, we still find the longitudinal ~~regions receive different amounts of shortwave radiation (PC = 0.876), temperature (PC = −0.219), precipitation (PC = 0.127), humidity (PC = 0.123), and vegetation greenness (PC = 0.382) (~~dependency of snow cover. Taking the SCD as an example, at a fixed elevation (e.g., 5000 m), a correlation still exists between longitude and SCD (R = 0.356, Figure 10b). ~~7), the southeast TP is warm and moist, and the northwest is cold and dry. Therefore, the further west on the TP, the longer the SCD, the earlier the SOD, and the later the SED (Figure 12a).~~ This implies that longitude could be interacting with additional factors to shape the spatial and temporal distribution of snow cover on the plateau. Vegetation greenness can change snow redistribution by intercepting the snow and regulating the balance of the solar radiation budget (Domine et al. 2016), vice versa, the processes and patterns of snow accumulation and melting affect vegetation greenness, species distribution, and community structure (Barrere et al., 2018). Most previous studies explored the response of vegetation greenness to snow cover, and the role of vegetation greenness on snow cover has rarely been investigated (Qi et al., 2021; Xu et al., 2022b). Our study showed that vegetation had mainly direct effects on snow cover, with particularly pronounced effects on SCD and SOD.

The dynamics of snow accumulation and melting are influenced by various factors. In addition to the factors analyzed in this paper, other factors may also play important roles in SP. Ground temperature primarily influences the structure and stability of snowpack by regulating energy exchange at the soil-snow interface (Rixin et al., 2022). As the ground temperature increases, the substrate absorbs additional thermal energy, which is conveyed to the base of the accumulated snow through heat conduction, resulting in melting of the lower snow layers. The heat from the warmer soil in the snow-free area can be transferred to the colder soil below the snow-covered area. Liquid water can also be transferred from the snow-free soil to the snow-covered soil, thus melting snow (Fassnacht et al., 2006). Therefore, soil properties (e.g., soil moisture) can also affect snow cover. In addition, atmospheric pollutants, especially those referred to as light-absorbing aerosols, such as black carbon, brown carbon and dust, can warm the atmosphere (Kang et al., 2019; Ji et al., 2015). After being deposited onto snowpack, these light-absorbing particles can reduce the surface albedos of snowpack and promote its melting (Zhang et al., 2018; Lau et al., 2018). Despite the potential importance of these factors to the SP of TP, they were not analyzed in this study due to limited data availability of these factors over extended spatial and temporal scales. Developing high-resolution, spatiotemporal continuous datasets for these factors will be useful in future efforts to comprehensively quantify the response of SP to changing climate conditions.

6 Conclusions

In this study, ~~based on the daily gap-free HMRFS-TP dataset,~~ we investigated the spatiotemporal ~~variation~~variability of SP on the TP from 2002 to ~~2021.~~2022 based on the daily gap-free HMRFS-TP dataset. We also quantified the direct and indirect effects of the associated factors on SP. The spatial patterns of SP were vertically zonal, with higher elevations having a longer SCD, earlier SOD, and later SED. ~~The interannual trends of all SP parameters varied in different zones (e.g., elevation and longitude) and contributed to the general trend in variation between 2002–2021: decreased SCD, delayed SOD, and slightly delayed SED. In particular, an elevation-dependent pattern of interannual variation in SP was observed below 5800 m. The direct and indirect effects of various associated factors on SP were analyzed in detail, among which meteorological factors had both direct and indirect effects; vegetation greenness had only a direct impact; and geographical location, topography, and atmospheric pollution had only indirect effects on SP. Undoubtedly, meteorological factors were the absolute dominant factors in particular temperature. However, the influences of topography, geographic location, vegetation greenness, and atmospheric pollution cannot be ignored.~~SCD had a statistically significant ($p < 0.1$) decreased trend in 4.62% of the TP at a mean rate of −1.74 days/year. SOD was significantly delayed in 2.34% of the TP at a mean rate of 2.90 days/year ($p < 0.1$), while SED was significantly advanced in 1.52% of the TP at a rate of −2.49 days/year ($p < 0.1$). Additionally, there exists a strong elevation dependence for the trend in SCD ($R = -0.73$), a moderate elevation dependence for the trend in SOD ($R = 0.59$), and no significant elevation dependence for the trend in SED ($R = 0.33$). Meteorological factors can directly affect SP as well as indirectly affect it by influencing the growth of vegetation, whereas the direct effect was much greater than the indirect effect. Geographical location and topographic conditions indirectly affected SP by modulating meteorological conditions and the growth of vegetation. Vegetation primarily influences SP by intercepting the snow and regulating the balance of the solar radiation budget. As two rather important factors, we identified that neither temperature nor precipitation showed consistently high importance as elevation increased.

This study explored the dynamic variation in snow cover and revealed the mediating effects of multiple factors in its changing process, which contributed to providing a strategic basis for predicting and solving the problems of climate change, hydrological cycle, and ecological balance in the future in the context of global warming on the TP.

Author contributions. JHX and YH designed and performed the experiments. YT and LXD performed the extraction of snow phenology. SJW, BLY, and JPW processed the validation experiments. ZJZ performed data curation. All the authors contributed to the analysis and writing of this paper.

Competing interests. The contact author has declared that neither they nor their co-authors have any competing interests.

Acknowledgements. This work was supported by the National Natural Science Foundation of China (no. 42071306). We would like to thank the National Meteorological Centre of China for providing the *in situ* observations over the Tibetan Plateau.

References

Bai, K., Li, K., Ma, M., Li, K., Li, Z., Guo, J., Chang, N.-B., Tan, Z., and Han, D.: LGHAP: the Long-term Gap-free High-resolution Air Pollutant concentration dataset, derived via tensor-flow-based multimodal data fusion, Earth System Science Data, 14, 907-927, https://doi.org/10.5194/essd-14-907-2022, 2022.

Barrere, M., Domine, F., Belke-Brea, M., and Sarrazin, D.: Snowmelt events in autumn can reduce or cancel the roil warming effect of snow–vegetation interactions in the Arctic, Journal of Climate, 31, 9507-9518, https://doi.org/10.1175/jcli-d-18-0135.1, 2018.

Cenfetelli, R. and Bassellier, G.: Interpretation of formative measurement in information systems research, MIS Quarterly, 33, 689-707, https://doi.org/10.2307/20650323, 2009.

Chen, W., Yao, T., Zhang, G., Li, F., Zheng, G., Zhou, Y., and Xu, F.: Towards ice-thickness inversion: an evaluation of global digital elevation models (DEMs) in the glacierized Tibetan Plateau, The Cryosphere, 16, 197-218, https://doi.org/10.5194/tc-16-197-2022, 2022.

Chen, X., Liang, S., Cao, Y., He, T., and Wang, D.: Observed contrast changes in snow cover phenology in northern middle and high latitudes from 2001-2014, Scientific Reports, 5, 16820, https://doi.org/10.1038/srep16820, 2015.

Chen, X., Long, D., Liang, S., He, L., Zeng, C., Hao, X., and Hong, Y.: Developing a composite daily snow cover extent record over the Tibetan Plateau from 1981 to 2016 using multisource data, Remote Sensing of Environment, 215, 284-299, https://doi.org/10.1016/j.rse.2018.06.021, 2018.

Cherkauer, K. A. and Sinha, T.: Time series analysis of soil freeze and thaw processes in Indiana, Journal of Hydrometeorology, 9, 936-950, https://doi.org/10.1175/2008jhm934.1, 2008.

Domine, F., Barrere, M., and Morin, S.: The growth of shrubs on high Arctic tundra at Bylot Island: impact on snow physical properties and permafrost thermal regime, Biogeosciences, 13, 6471-6486, https://doi.org/10.5194/bg-13-6471-2016, 2016.

Fan, X., Gu, Y., Liou, K.-N., Lee, W.-L., Zhao, B., Chen, H., and Lu, D.: Modeling study of the impact of complex terrain on the surface energy and hydrology over the Tibetan Plateau, Climate Dynamics, 53, 6919-6932, https://doi.org/10.1007/s00382-019-04966-z, 2019.

Fassnacht, S. R., Yang Z. L., Snelgrove, K. R., Soulis, E. D., and Kouwen, N.: Effects of Averaging and Separating Soil Moisture and Temperature in the Presence of Snow Cover in a SVAT and Hydrological Model for a Southern Ontario, Canada, Watershed, Journal of Hydrometeorology, 7, 298–304, https://doi.org/10.1175/JHM489.1, 2006.

Fyfe, J. C., Derksen, C., Mudryk, L., Flato, G. M., Santer, B. D., Swart, N. C., Molotch, N. P., Zhang, X., Wan, H., Arora, V. K., Scinocca, J., and Jiao, Y.: Large near-term projected snowpack loss over the western United States, Nature Communications, 8, 14996, https://doi.org/10.1038/ncomms14996, 2017.

Grace, J. B., Anderson, T. M., Olff, H., and Scheiner, S. M.: On the specification of structural equation models for ecological systems, Ecological Monographs, 80, 67-87, https://doi.org/10.1890/09-0464.1, 2010.

Guo, H., Wang, X., Guo, Z., and Chen, S.: Assessing snow phenology and its environmental driving factors in Northeast China, Remote Sensing, 14, https://doi.org/10.3390/rs14020262, 2022.

Gutzler, D. S. and Rosen, R. D.: Interannual variability of wintertime snow cover across the Northern Hemisphere, Journal of Climate, 5, https://doi.org/10.1175/1520-0442(1992)005<1441:IVOWSC>2.0.CO;2, 1992.

Hair, J. F., Black, W. C., Babin, B. J., and Anderson, R. E.: Multivariate data analysis (7th ed.), Englewood Cliffs: Prentice Hall, 2010.

Hair, J. F., Sarstedt, M., Ringle, C. M., and Mena, J. A.: An assessment of the use of partial least squares structural equation modeling in marketing research, Journal of the Academy of Marketing Science, 40, 414-433, https://doi.org/10.1007/s11747-011-0261-6, 2011.

Hall, D. K., Riggs, G., and Salomonson, V. V.: Development of methods for mapping global snow cover using Moderate Resolution Imaging Spectroradiometer (MODIS) data, Remote Sensing of Environment, 54, 127-140, https://doi.org/10.1016/0034-4257(95)00137-P, 1995.

Hao, X., Zhao, Q., Ji, W., Wang, J., and Li, H.: A dataset of snow cover phenology in China based on AVHRR from 1980 to 2020, China Scientific Data, 7, https://doi.org/10.11922/11-6035.ncdc.2021.0026.zh, 2022.

He, J., Yang, K., Tang, W., Lu, H., Qin, J., Chen, Y., and Li, X.: The first high-resolution meteorological forcing dataset for land process studies over China, Scientific Data, 7, 25, https://doi.org/10.1038/s41597-020-0369-y, 2020.

Hirsch, R. M., Slack, J. R., and Smith, R. A.: Techniques of trend analysis for monthly water-quality data, Water Resources Research, 18, 107-121, https://doi.org/10.1029/WR018i001p00107, 1982.

Huang, X., Deng, J., Wang, W., Feng, Q., and Liang, T.: Impact of climate and elevation on snow cover using integrated remote sensing snow products in Tibetan Plateau, Remote Sensing of Environment, 190, 274-288, https://doi.org/10.1016/j.rse.2016.12.028, 2017.

Huang, X., Liu, C., Zheng, Z., Wang, Y., Li, X., and Liang, T.: Snow cover variations across China from 1951-2018, https://doi.org/10.5194/tc-2020-202, 2020.

Huang, Y., Liu, H., Yu, B., Wu, J., Kang, E. L., Xu, M., Wang, S., Klein, A., and Chen, Y.: Improving MODIS snow products with a HMRF-based spatio-temporal modeling technique in the Upper Rio Grande Basin, Remote Sensing of Environment, 204, 568-582, https://doi.org/10.1016/j.rse.2017.10.001, 2018.

Huang, Y., Song, Z. C., Yang, H. X., Yu, B. L., Liu, H. X., Che, T., Chen, J., Wu, J. P., Shu, S., Peng, X. B., Zheng, Z. J., and Xu, J. H.: Snow cover detection in mid-latitude mountainous and polar regions using nighttime light data, Remote Sensing of Environment, 268, https://doi.org/10.1016/j.rse.2021.112766, 2022a.

Huang, Y., Xu, J., Xu, J., Zhao, Y., Yu, B., Liu, H., Wang, S., Xu, W., Wu, J., and Zheng, Z.: HMRFS–TP: long-term daily gap-free snow cover products over the Tibetan Plateau from 2002 to 2021 based on hidden Markov random field model, Earth System Science Data, 14, 4445-4462, https://doi.org/10.5194/essd-14-4445-2022, 2022b.

~~Ishida, K., Ohara, N., Ercan, A., Jang, S., Trinh, T., Kavvas, M. L., Carr, K., and Anderson, M. L.: Impacts of climate change on snow accumulation and melting processes over mountainous regions in Northern California during the 21st century, Science of the Total Environment, 685, 104-115, https://doi.org/10.1016/j.scitotenv.2019.05.255, 2019.~~

Jain, S. K., Goswami, A., and Saraf, A. K.: Role of elevation and aspect in snow distribution in Western Himalaya, Water Resources Management, 23, 71-83, https://doi.org/10.1007/s11269-008-9265-5, 2008.

Ji, Z., Kang, S., Cong, Z., Zhang, Q., Yao, T.: Simulation of carbonaceous aerosols over the third pole and adjacent regions: distribution, transportation, deposition, and climatic effects, Climate Dynamics, 45 (9), 2831–2846, https://doi.org/10.1007/s00382-015-2509-1, 2015.

Kang, S., Zhang, Q., Qian, Y., Ji, Z., Li, C., Cong, Z., Zhang, Y., Guo, J., Du, W., Huang, J., You, Q., Panday, A. K., Rupakheti, M., Chen, D., Gustafsson, O., Thiemens, M. H., and Qin, D.: Linking atmospheric pollution to cryospheric change in the Third Pole region: current progress and future prospects, National Science Review, 6, 796-809, https://doi.org/10.1093/nsr/nwz031, 2019.

Keyser, S. R., Fink, D., Gudex-Cross, D., Radeloff, V. C., Pauli, J. N., and Zuckerberg, B.: Snow cover dynamics: an overlooked yet important feature of winter bird occurrence and abundance across the United States, Ecography, 2023, https://doi.org/10.1111/ecog.06378, 2022.

Kraaijenbrink, P. D. A., Stigter, E. E., Yao, T., and Immerzeel, W. W.: Climate change decisive for Asia's snow meltwater supply, Nature Climate Change, 11, 591-597, https://doi.org/10.1038/s41558-021-01074-x, 2021.

Lau, W. and Kim, K.-M.: Impact of Snow Darkening by Deposition of Light-Absorbing Aerosols on Snow Cover in the Himalayas–Tibetan Plateau and Influence on the Asian Summer Monsoon: A Possible Mechanism for the Blanford Hypothesis, Atmosphere, 9, https://doi.org/10.1007/10.3390/atmos9110438, 2018.

Li, H., Wang, J., Hao, X.: Influence of Blowing Snow on Snow Mass and Energy Exchanges in the Qilian Mountainous, Journal of Glaciology and Geocryology, 34(05),1084-1090, 2012. (in Chinese)

Li, K., Li, H., Wang, L., and Gao, W.: On the relationship between local topography and small glacier change under climatic warming on Mt. Bogda, Eastern Tian Shan, China, J Earth Sci-China, 22, 515-527, https://doi.org/10.1007/s12583-011-0204-7, 2011.

Li, W., Chen, J., Li, L., Orsolini, Y. J., Xiang, Y., Senan, R., and de Rosnay, P.: Impacts of snow assimilation on seasonal snow and meteorological forecasts for the Tibetan Plateau, The Cryosphere, 16, 4985-5000, https://doi.org/10.5194/tc-16-4985-2022, 2022.

Li, W., Qiu, B., Guo, W., Zhu, Z., and Hsu, P. C.: Intraseasonal variability of Tibetan Plateau snow cover, International Journal of Climatology, 40, 3451-3466, https://doi.org/10.1002/joc.6407, 2019.

Lopatin, J., Kattenborn, T., Galleguillos, M., Perez-Quezada, J. F., and Schmidtlein, S.: Using aboveground vegetation attributes as proxies for mapping peatland belowground carbon stocks, Remote Sensing of Environment, 231, https://doi.org/10.1016/j.rse.2019.111217, 2019.

Ma, H., Zhang, G., Mao, R., Su, B., Liu, W., and Shi, P.: Snow depth variability across the Qinghai Plateau and its influencing factors during 1980–2018, International Journal of Climatology, 43, 1094-1111, https://doi.org/10.1002/joc.7883, 2022.

Ma, N., Yu, K., Zhang, Y., Zhai, J., Zhang, Y., and Zhang, H.: Ground observed climatology and trend in snow cover phenology across China with consideration of snow-free breaks, Climate Dynamics, 55, 2867-2887, https://doi.org/10.1007/s00382-020-05422-z, 2020.

Ma, Q., Keyimu, M., Li, X., Wu, S., Zeng, F., and Lin, L.: Climate and elevation control snow depth and snow phenology on the Tibetan Plateau, Journal of Hydrology, 617, https://doi.org/10.1016/j.jhydrol.2022.128938, 2023.

Moran-Tejeda, E., Lopez-Moreno, J. I., and Beniston, M.: The changing roles of temperature and precipitation on snowpack variability in Switzerland as a function of altitude, Geophysical Research Letters, 40, 2131-2136, https://doi.org/10.1002/grl.50463, 2013.

Notarnicola, C.: Hotspots of snow cover changes in global mountain regions over 2000–2018, Remote Sensing of Environment, 243, https://doi.org/10.1016/j.rse.2020.111781, 2020.

~~Peng, S., Ding, Y., Liu, W., and Li, Z.: 1 km monthly temperature and precipitation dataset for China from 1901 to 2017, Earth System Science Data, 11, 1931-1946, https://doi.org/10.5194/essd-11-1931-2019, 2019.~~

Pulliainen, J., Luojus, K., Derksen, C., Mudryk, L., Lemmetyinen, J., Salminen, M., Ikonen, J., Takala, M., Cohen, J., Smolander, T., and Norberg, J.: Patterns and trends of Northern Hemisphere snow mass from 1980 to 2018, Nature, 581, 294-298, https://doi.org/10.1038/s41586-020-2258-0, 2020.

Qi, Y., Wang, H., Ma, X., Zhang, J., and Yang, R.: Relationship between vegetation phenology and snow cover changes during 2001–2018 in the Qilian Mountains, Ecological Indicators, 133, https://doi.org/10.1016/j.ecolind.2021.108351, 2021.

Ren, Y., Liu, S.: Different influences of temperature on snow cover and sea ice area in the Northern Hemisphere, Geographical Research, 37(05), 870-882, 2018. (in Chinese)

Rixen, C., Høye, T. T., Macek, P., Aerts, R., Alatalo, J. M., Anderson, J. T., Arnold, P. A., Barrio, I. C., Bjerke, J. W., Björkman, M. P., Blok, D., Blume-Werry, G., Boike, J., Bokhorst, S., Carbognani, M., Christiansen, C. T., Convey, P., Cooper, E. J., Cornelissen, J. H. C., Coulson, S. J., Dorrepaal, E., Elberling, B., Elmendorf, S. C., Elphinstone, C., Forte, T. a. G. W., Frei, E. R., Geange, S. R., Gehrmann, F., Gibson, C., Grogan, P., Halbritter, A. H., Harte, J., Henry, G. H. R., Inouye, D. W., Irwin, R. E., Jespersen, G., Jónsdóttir, I. S., Jung, J. Y., Klinges, D. H., Kudo, G., Lämsä, J., Lee, H., Lembrechts, J. J., Lett, S., Lynn, J. S., Mann, H. M. R., Mastepanov, M., Morse, J., Myers-Smith, I. H., Olofsson, J., Paavola, R., Petraglia, A., Phoenix, G. K., Semenchuk, P., Siewert, M. B., Slatyer, R., Spasojevic, M. J., Suding, K., Sullivan, P., Thompson, K. L., Väisänen, M., Vandvik, V., Venn, S., Walz, J., Way, R., Welker, J. M., Wipf, S., and Zong, S.: Winters are changing: snow effects on Arctic and alpine tundra ecosystems, Arctic Science, 8, 572-608, 10.1139/as-2020-0058, 2022.

Ringle, Sarstedt, and Straub: Editor's comments: a critical look at the use of PLS-SEM in "MIS Quarterly", MIS Quarterly, 36, https://doi.org/10.2307/41410402, 2012.

Scalzitti, J., Strong, C., and Kochanski, A.: Climate change impact on the roles of temperature and precipitation in western U.S. snowpack variability, Geophysical Research Letters, 43, 5361-5369, https://doi.org/10.1002/2016gl068798, 2016.

Sen, P. K.: Estimates of the regression coefficient based on Kendall's Tau, Journal of the American Statistical Association, 63, 1379-1389, https://doi.org/10.1080/01621459.1968.10480934, 1968.

Shen, M., Wang, S., Jiang, N., Sun, J., Cao, R., Ling, X., Fang, B., Zhang, L., Zhang, L., Xu, X., Lv, W., Li, B., Sun, Q., Meng, F., Jiang, Y., Dorji, T., Fu, Y., Iler, A., Vitasse, Y., Steltzer, H., Ji, Z., Zhao, W., Piao, S., and Fu, B.: Plant phenology changes and drivers on the Qinghai–Tibetan Plateau, Nature Reviews Earth & Environment, 3, 633-651, https://doi.org/10.1038/s43017-022-00317-5, 2022.

Sturm, M., Holmgren, J., McFadden, J. P., Liston, G. E., Chapin, F. S., and Racine, C. H.: Snow–shrub interactions in Arctic Tundra: a hypothesis with climatic implications, Journal of Climate, 14, 336-344, https://doi.org/10.1175/1520-0442(2001)014<0336:Ssiiat>2.0.Co;2, 2001.

Tang, Z., Deng, G., Hu, G., Zhang, H., Pan, H., and Sang, G.: Satellite observed spatiotemporal variability of snow cover and snow phenology over high mountain Asia from 2002 to 2021, Journal of Hydrology, 613, https://doi.org/10.1016/j.jhydrol.2022.128438, 2022.

Tarca, G., Guglielmin, M., Convey, P., Worland, M. R., and Cannone, N.: Small-scale spatial–temporal variability in snow cover and relationships with vegetation and climate in maritime Antarctica, Catena, 208, https://doi.org/10.1016/j.catena.2021.105739, 2022.

Theil, H.: A rank-invariant method of linear and polynomial regression analysis, Springer Netherlands, 1992.

Venturini, S. and Mehmetoglu, M.: plssem: a stata package for structural equation modeling with partial least squares, Journal of Statistical Software, 88, https://doi.org/10.18637/jss.v088.i08, 2019.

Vermote, E.: MODIS/Terra Surface Reflectance 8-Day L3 Global 500m SIN Grid V061. NASA EOSDIS Land Processes Distributed Active Archive Center, 2021.

~~Walker, D. A., Halfpenny, J. C., Walker, M. D., and Wessman, C. A.: Long-Term studies of snow-vegetation interactions, BioScience, 43, 287-301, https://doi.org/10.2307/1312061, 1993.~~

Wang, H., Zhang, X., Xiao, P., Zhang, K., and Wu, S.: Elevation-dependent response of snow phenology to climate change from a remote sensing perspective: A case survey in the central Tianshan mountains from 2000 to 2019, International Journal of Climatology, https://doi.org/10.1002/joc.7330, 2021.

Wang, X., Wu, C., Wang, H., Gonsamo, A., and Liu, Z.: No evidence of widespread decline of snow cover on the Tibetan Plateau over 2000-2015, Scientific Reports, 7, 14645, https://doi.org/10.1038/s41598-017-15208-9, 2017.

Wang, X., Zhong, L., and Ma, Y.: Estimation of 30 m land surface temperatures over the entire Tibetan Plateau based on Landsat-7 ETM+ data and machine learning methods, International Journal of Digital Earth, 15, 1038-1055, https://doi.org/10.1080/17538947.2022.2088873, 2022.

Wang, Z., Huang, L., and Shao, M. a.: Spatial variations and influencing factors of soil organic carbon under different land use types in the alpine region of Qinghai-Tibet Plateau, Catena, 220, https://doi.org/10.1016/j.catena.2022.106706, 2023.

Wu, G., Duan, A., Liu, Y., Mao, J., Ren, R., Bao, Q., He, B., Liu, B., and Hu, W.: Tibetan Plateau climate dynamics: recent research progress and outlook, National Science Review, 2, 100-116, https://doi.org/10.1093/nsr/nwu045, 2015.

Xie, Z., Hu, Z., Gu, L., Sun, G., Du, Y., and Yan, X.: Meteorological forcing datasets for blowing snow modeling on the Tibetan Plateau: evaluation and intercomparison, Journal of Hydrometeorology, 18, 2761-2780, https://doi.org/10.1175/jhm-d-17-0075.1, 2017.

~~Xu, H., Ren, Y., Zhang, W., Meng, W., Yun, X., Yu, X., Li, J., Zhang, Y., Shen, G., Ma, J., Li, B., Cheng, H., Wang, X., Wan, Y., and Tao, S.: Updated global black carbon emissions from 1960 to 2017: improvements, trends, and drivers, Environment Science Technology, 55, 7869-7879, https://doi.org/10.1021/acs.est.1c03117, 2021.~~

Xu, J., Tang, Y., Xu, J., Chen, J., Bai, K., Shu, S., Yu, B., Wu, J., and Huang, Y.: Evaluation of vegetation indexes and green-up date extraction methods on the Tibetan Plateau, Remote Sensing, 14, https://doi.org/10.3390/rs14133160, 2022a.

Xu, J., Tang, Y., Xu, J., Shu, S., Yu, B., Wu, J., and Huang, Y.: Impact of snow cover phenology on the vegetation green-up date on the Tibetan Plateau, Remote Sensing, 14, https://doi.org/10.3390/rs14163909, 2022b.

Yang, W., Kobayashi, H., Wang, C., Shen, M., Chen, J., Matsushita, B., Tang, Y., Kim, Y., Bret-Harte, M. S., Zona, D., Oechel, W., and Kondoh, A.: A semi-analytical snow-free vegetation index for improving estimation of plant phenology in tundra and grassland ecosystems, Remote Sensing of Environment, 228, 31-44, https://doi.org/10.1016/j.rse.2019.03.028, 2019.

Yang, K., Jiang, Y., Tang, W., He, J., Shao, C., Zhou, X., Lu, H., Chen, Y., Li, X., Shi, J.: A high-resolution near-surface meteorological forcing dataset for the Third Pole region (TPMFD, 1979-2022), National Tibetan Plateau/Third Pole Environment Data Center, https://doi.org/10.11888/Atmos.tpdc.300398, 2023.

Yao, T., Thompson, L. G., Mosbrugger, V., Zhang, F., Ma, Y., Luo, T., Xu, B., Yang, X., Joswiak, D. R., Wang, W., Joswiak, M. E., Devkota, L. P., Tayal, S., Jilani, R., and Fayziev, R.: Third Pole Environment (TPE), Environmental Development, 3, 52-64, 10.1016/j.envdev.2012.04.002, 2012.

You, Q., Cai, Z., Pepin, N., Chen, D., Ahrens, B., Jiang, Z., Wu, F., Kang, S., Zhang, R., Wu, T., Wang, P., Li, M., Zuo, Z., Gao, Y., Zhai, P., and Zhang, Y.: Warming amplification over the Arctic Pole and Third Pole: trends, mechanisms and consequences, Earth-Science Reviews, 217, https://doi.org/10.1016/j.earscirev.2021.103625, 2021.

You, Q., Wu, T., Shen, L., Pepin, N., Zhang, L., Jiang, Z., Wu, Z., Kang, S., and AghaKouchak, A.: Review of snow cover variation over the Tibetan Plateau and its influence on the broad climate system, Earth-Science Reviews, 201, https://doi.org/10.1016/j.earscirev.2019.103043, 2020.

Zhang, H., Immerzeel, W. W., Zhang, F., de Kok, R. J., Chen, D., and Yan, W.: Snow cover persistence reverses the altitudinal patterns of warming above and below 5000 m on the Tibetan Plateau, Science of the Total Environment, 803, 149889, https://doi.org/10.1016/j.scitotenv.2021.149889, 2022.

Zhang, Y., Kang, S., Sprenger, M., Cong, Z., Gao, T., Li, C., Tao, S., Li, X., Zhong, X., Xu, M., Meng, W., Neupane, B., Qin, X., and Sillanpää, M.: Black carbon and mineral dust in snow cover on the Tibetan Plateau, The Cryosphere, 12, 413-431, https://doi.org/10.5194/tc-12-413-2018, 2018.

Zhao, Q., Hao, X., Wang, J., Sun, X., and Li, H.: A dataset of snow cover phenology in China based on MODIS during 2000–2020, China Scientific Data, 7, https://doi.org/10.11922/11-6035.ncdc.2021.0027.zh, 2022.

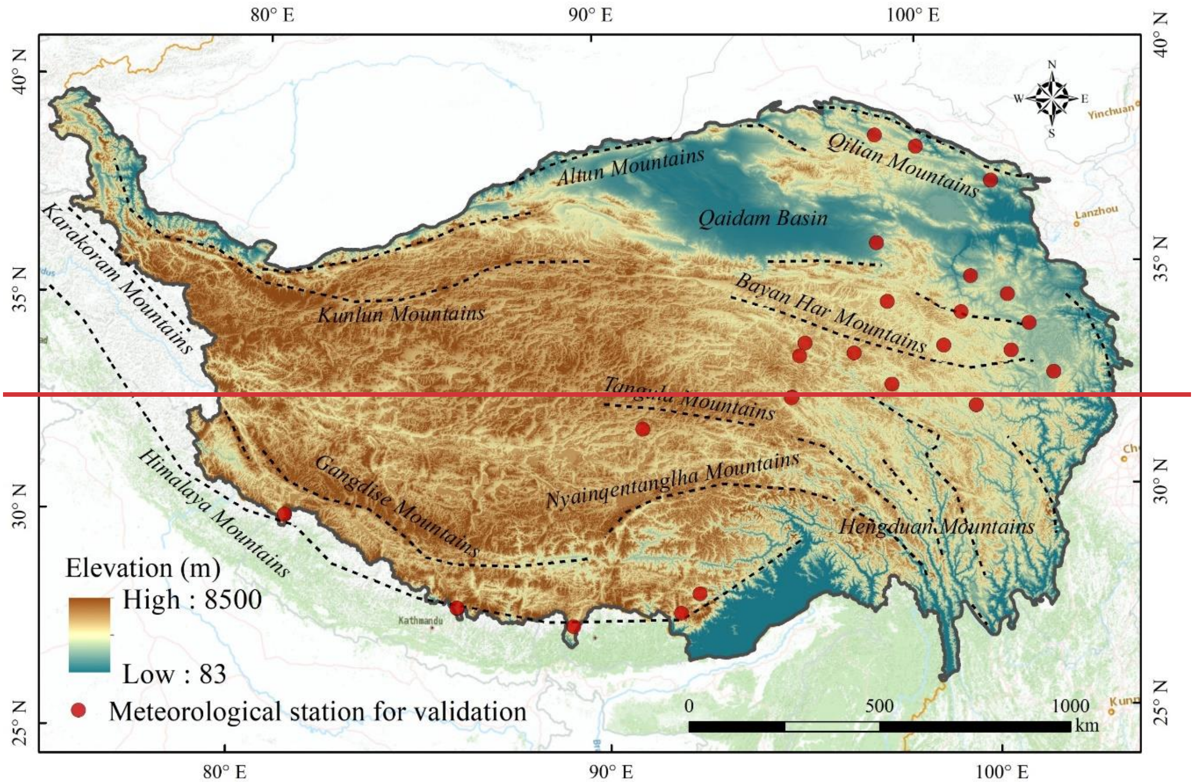
80° E
90° E
100° E
40° N
35° N
30° N
25° N
N
S
W
E
Yinchuan
Lanzhou
Kathmandu
Qilian Mountains
Altun Mountains
Qaidam Basin
Karakoram Mountains
Kunlun Mountains
Bayan Har Mountains
Tangula Mountains
Gangdise Mountains
Nyainqentanglha Mountains
Himalaya Mountains
Hengduan Mountains
Elevation (m)
High : 8500
Low : 83
Meteorological station for validation
0
500
1000
km

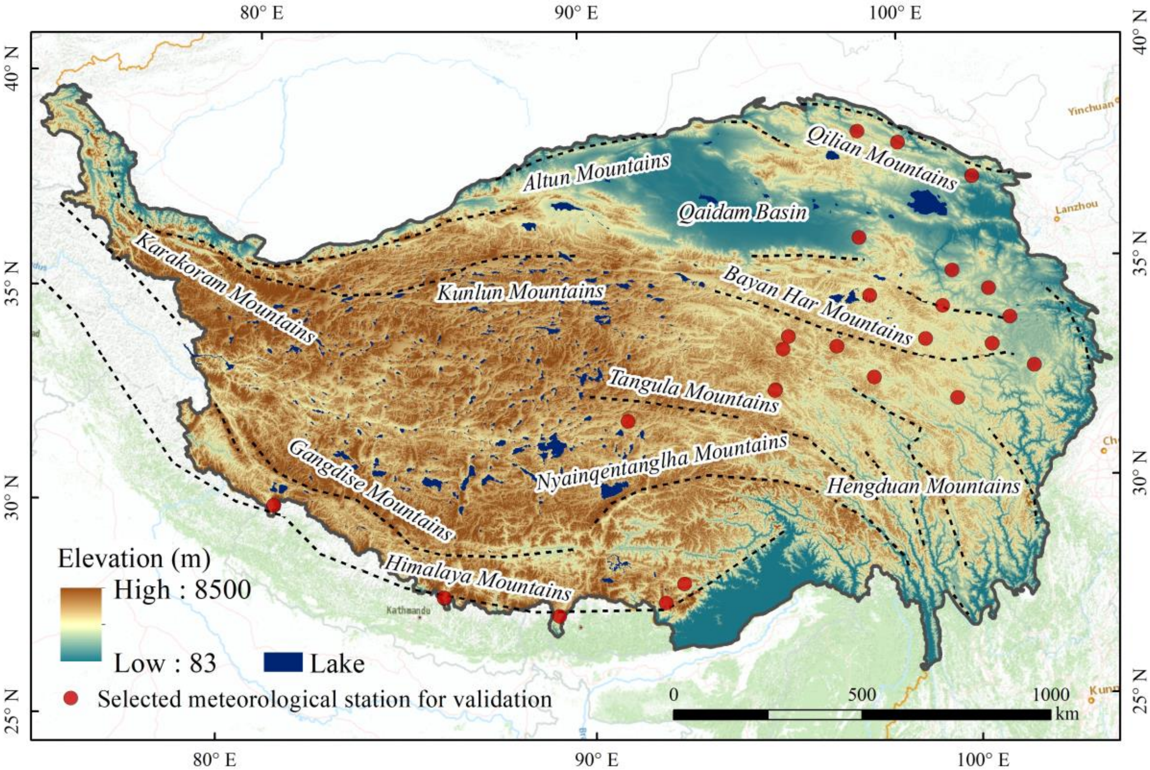

Figure 1: Topography, lakes and distribution of selected meteorological stations for validation on the Tibetan Plateau (TP) ~~used for data validation~~ (base map from ESRI).

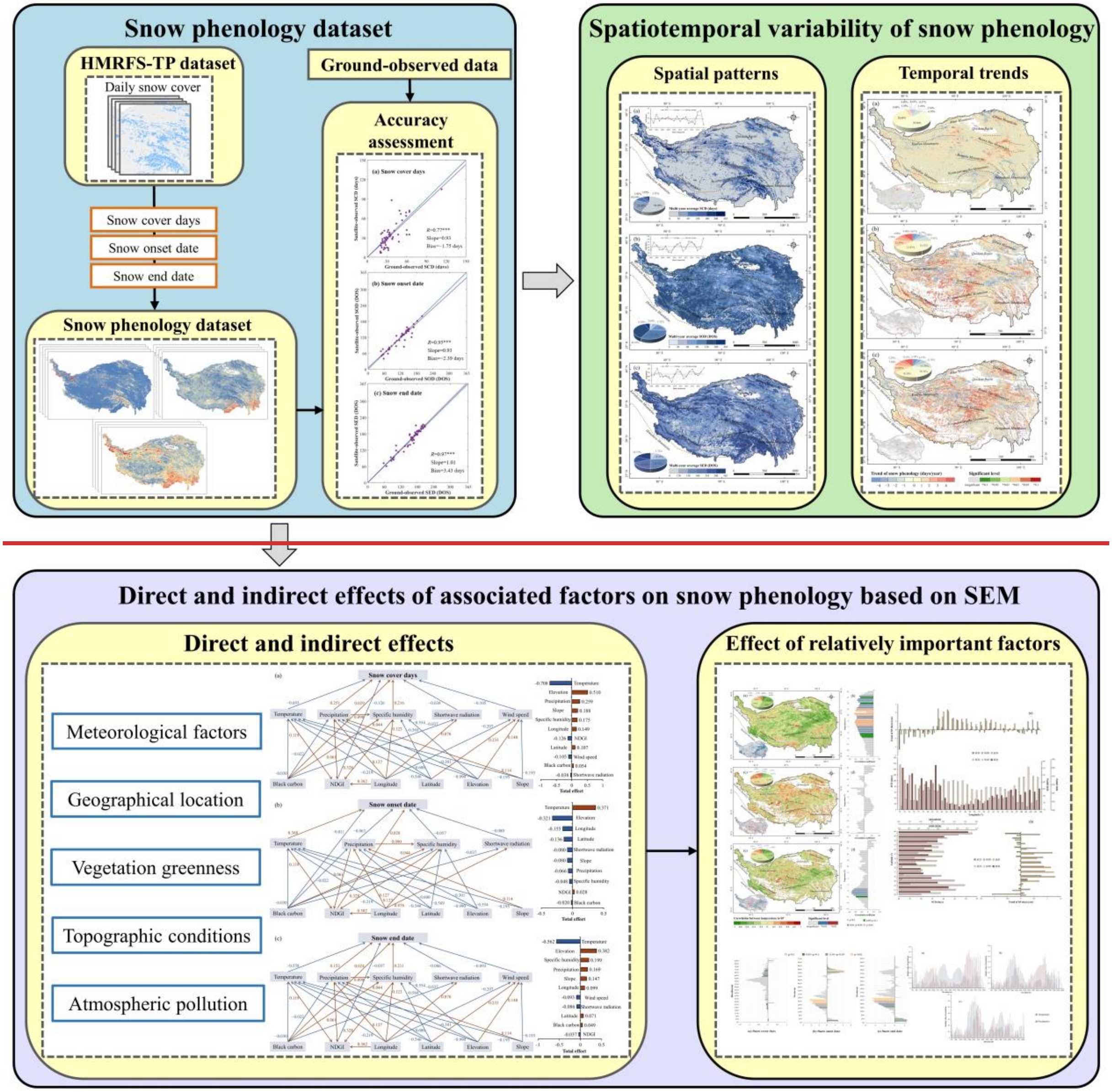
Snow phenology dataset
HMRFS-TP dataset
Daily snow cover
Ground-observed data
Accuracy assessment
Snow cover days
Snow onset date
Snow end date
Snow phenology dataset
Spatiotemporal variability of snow phenology
Spatial patterns
Temporal trends
Direct and indirect effects of associated factors on snow phenology based on SEM
Direct and indirect effects
Meteorological factors
Geographical location
Vegetation greenness
Topographic conditions
Atmospheric pollution
Effect of relatively important factors

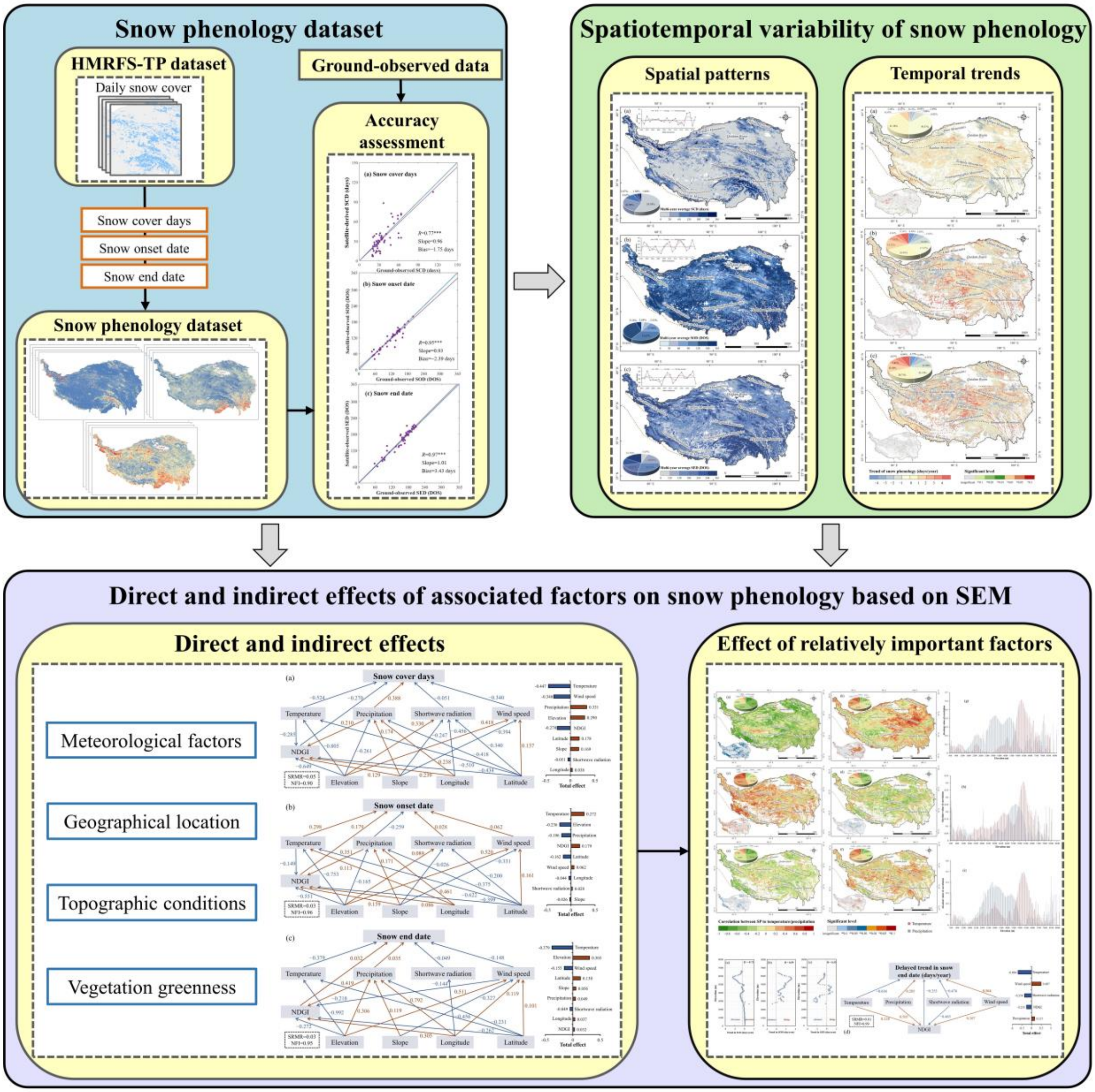

Figure 2: Flowchart to reveal the spatiotemporal variability of snow phenology (SP) and the direct and indirect effects of associated factors on the TP from 2002 to ~~2021~~2022. SEM refers to the Structural Equation Model.

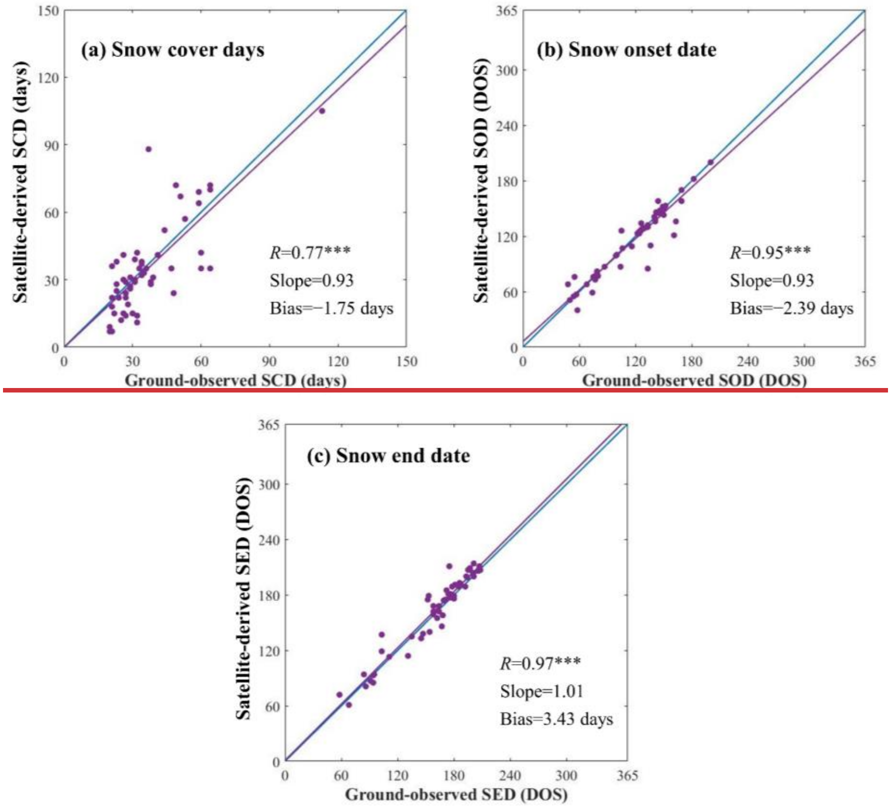
(a) Snow cover days
Satellite-derived SCD (days)
Ground-observed SCD (days)
R=0.77***
Slope=0.93
Bias=−1.75 days
(b) Snow onset date
Satellite-derived SOD (DOS)
Ground-observed SOD (DOS)
R=0.95***
Slope=0.93
Bias=−2.39 days
(c) Snow end date
Satellite-derived SED (DOS)
Ground-observed SED (DOS)
R=0.97***
Slope=1.01
Bias=3.43 days

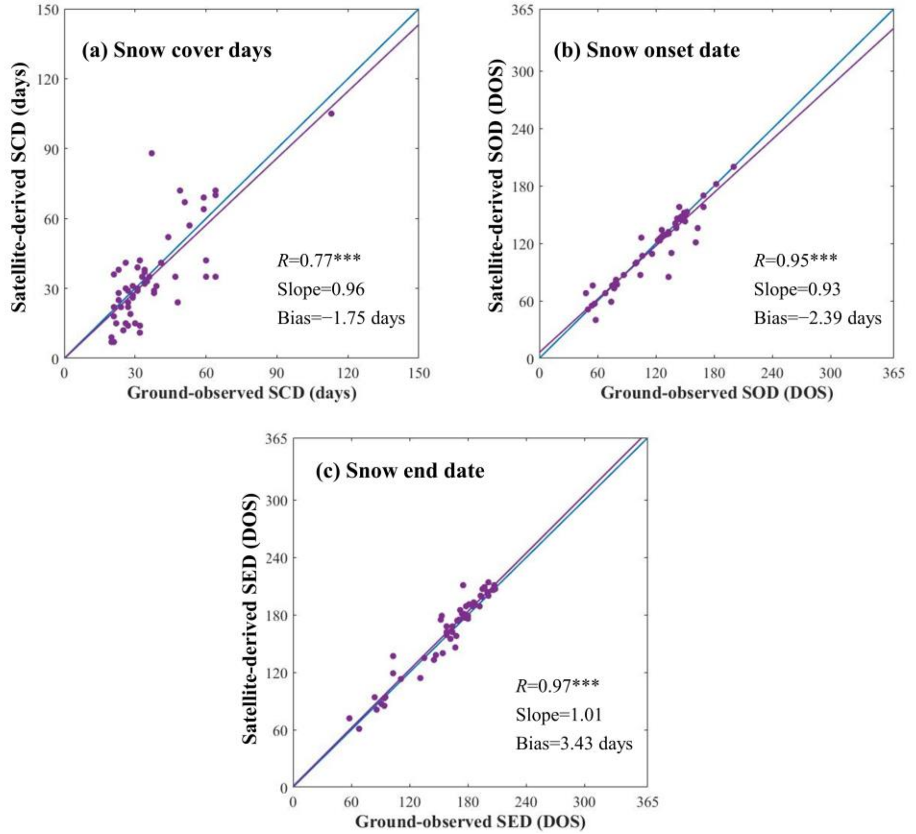

Figure 3: The accuracy of SP parameters of (a) SCD, (b) SOD, and (c) SED evaluated by ground-observed values from 2002 to ~~2021. (a) SCD, (b) SOD, and (c) SED~~2022. Note: SCD, SOD, and SED denote snow cover days, snow onset date, and snow end date, respectively. DOS represents the day of the snow season. * indicates significance at the level of 0.01.~~ DOS represents the day of the snow season.~~**

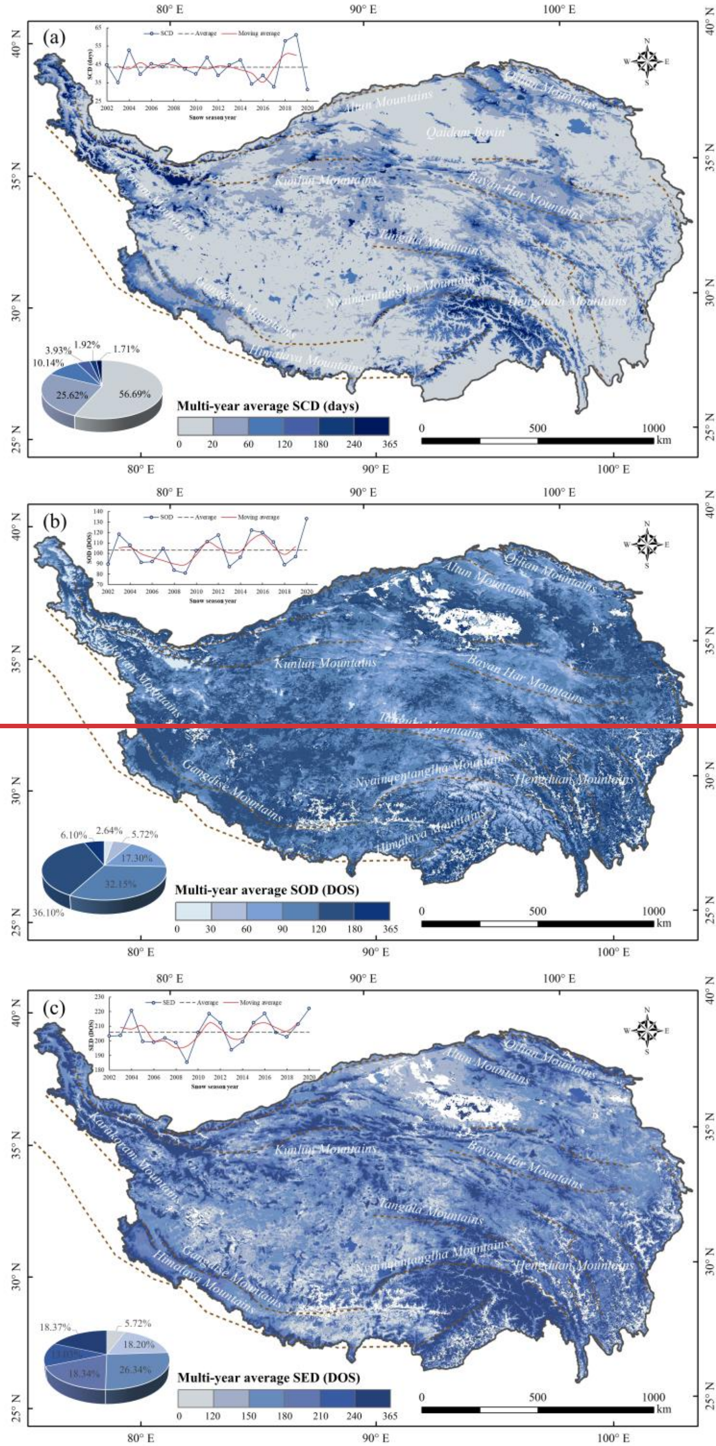
(a)
Multi-year average SCD (days)
0 20 60 120 180 240 365
56.69%
25.62%
10.14%
3.93%
1.92%
1.71%
Qilian Mountains
Altun Mountains
Qaidam Basin
Kunlun Mountains
Bayan Har Mountains
Tanggula Mountains
Nyainqentanglha Mountains
Hengduan Mountains
Gangdise Mountains
Himalaya Mountains
Karakoram Mountains
(b)
Multi-year average SOD (DOS)
0 30 60 90 120 180 365
36.10%
32.15%
17.30%
6.10%
5.72%
2.64%
(c)
Multi-year average SED (DOS)
0 120 150 180 210 240 365
26.34%
18.37%
18.34%
18.20%
5.72%
80° E
90° E
100° E
25° N
30° N
35° N
40° N
0 500 1000 km
Snow season year

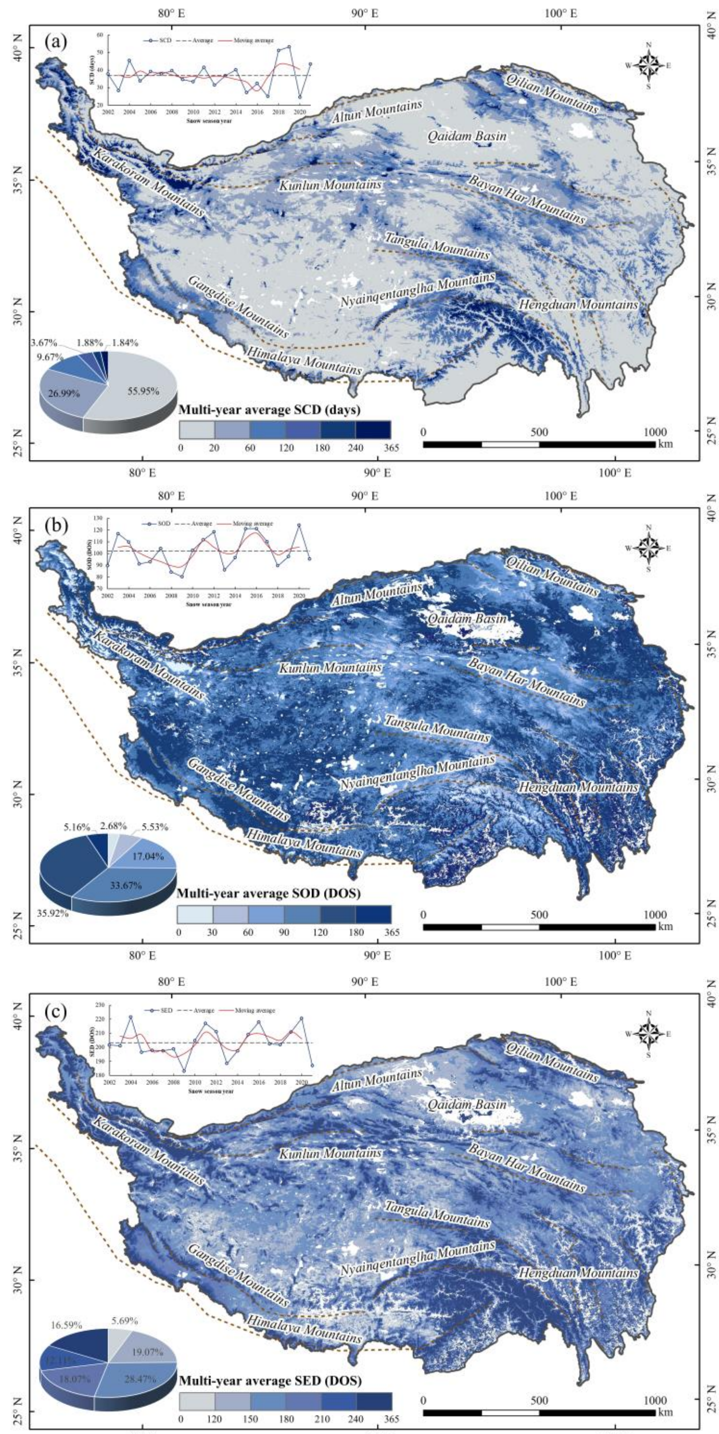
(a)
SCD
Average
Moving average
Snow season year
Altun Mountains
Qilian Mountains
Qaidam Basin
Karakoram Mountains
Kunlun Mountains
Bayan Har Mountains
Tangula Mountains
Nyainqentanglha Mountains
Gangdise Mountains
Hengduan Mountains
Himalaya Mountains
3.67%
1.88%
1.84%
9.67%
26.99%
55.95%
Multi-year average SCD (days)
0 20 60 120 180 240 365
0 500 1000 km
(b)
SOD
Average
Moving average
Snow season year
Altun Mountains
Qilian Mountains
Qaidam Basin
Karakoram Mountains
Kunlun Mountains
Bayan Har Mountains
Tangula Mountains
Nyainqentanglha Mountains
Gangdise Mountains
Hengduan Mountains
Himalaya Mountains
5.16%
2.68%
5.53%
17.04%
33.67%
35.92%
Multi-year average SOD (DOS)
0 30 60 90 120 180 365
0 500 1000 km
(c)
SED
Average
Moving average
Snow season year
Altun Mountains
Qilian Mountains
Qaidam Basin
Karakoram Mountains
Kunlun Mountains
Bayan Har Mountains
Tangula Mountains
Nyainqentanglha Mountains
Gangdise Mountains
Hengduan Mountains
Himalaya Mountains
16.59%
5.69%
19.07%
18.07%
28.47%
Multi-year average SED (DOS)
0 120 150 180 210 240 365
0 500 1000 km
80° E
90° E
100° E
25° N
30° N
35° N
40° N

Figure 4: The spatial pattern of the multiyear averaged SP of (a) SCD, (b) SOD, and (c) SED on the TP from 2002 to ~~2021. (a) SCD, (b) SOD, and (c) SED~~2022. Note: pixels ~~which have~~ not ~~been~~ detected ~~in 19~~for 20 years ~~are regarded~~or identified as lake area were considered as snow-free pixels (i.e., the white area in the figure).

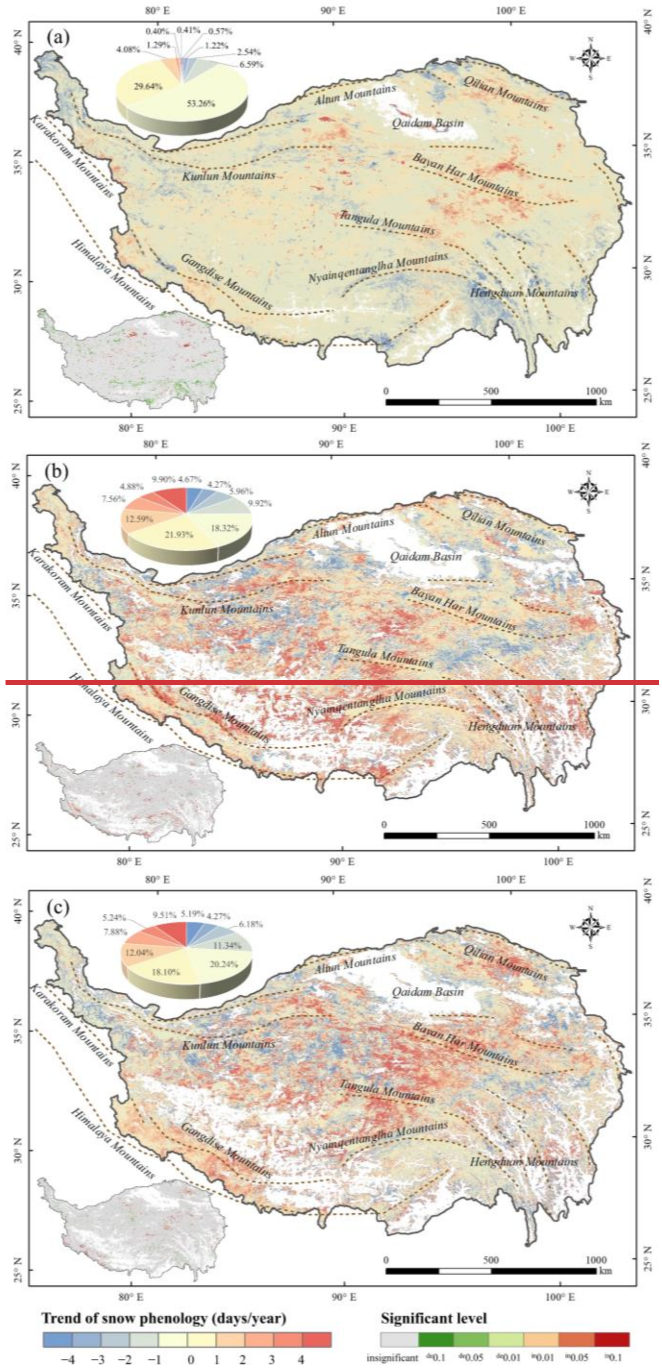

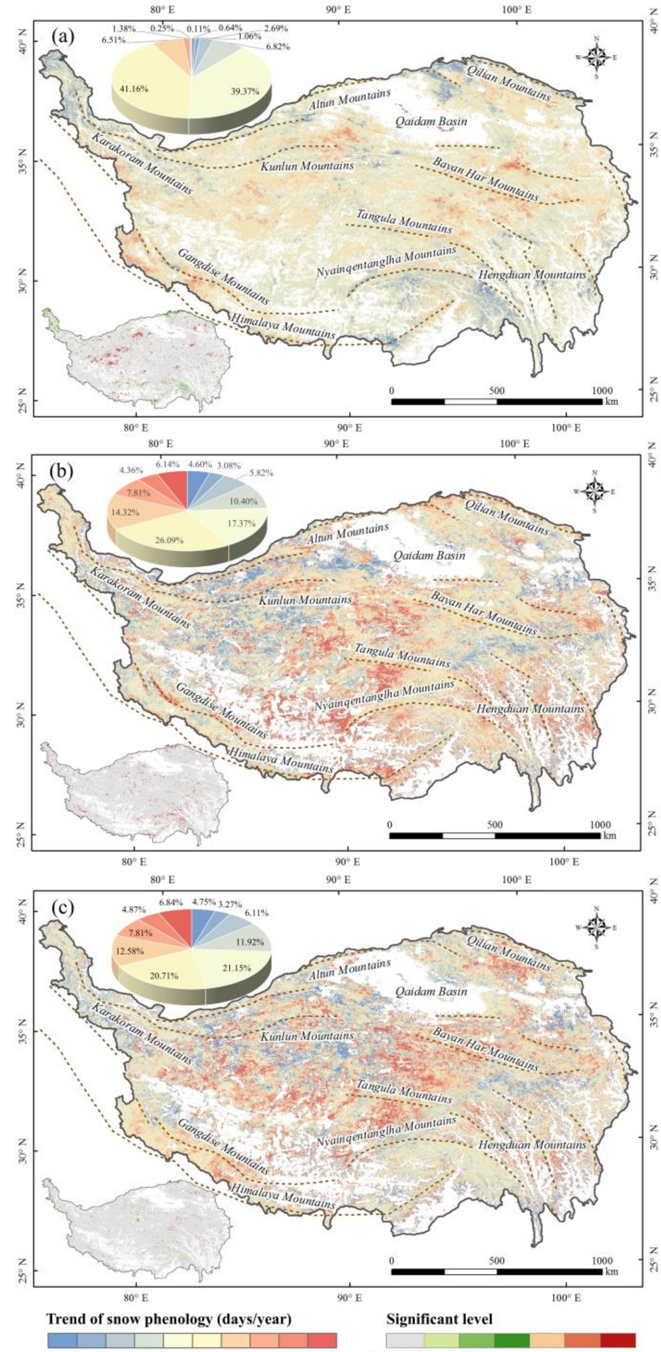

Figure 5: ~~Interannual variation trend of~~Trends in SP of (a) SCD, (b) SOD, and (c) SED on the ~~SP~~TP from 2002 to ~~2021. (a) SCD, (b) SOD, and (c) SED~~2022. Note: the map at the bottom left of each subgraph indicates the significant level. The symbol "de" in the legend indicates a significantly decreased trend and "in" indicates a significantly increased trend.

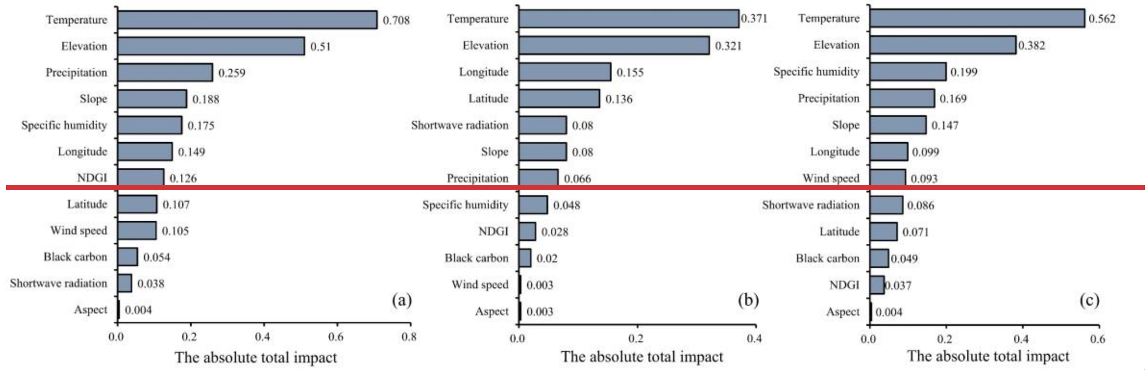

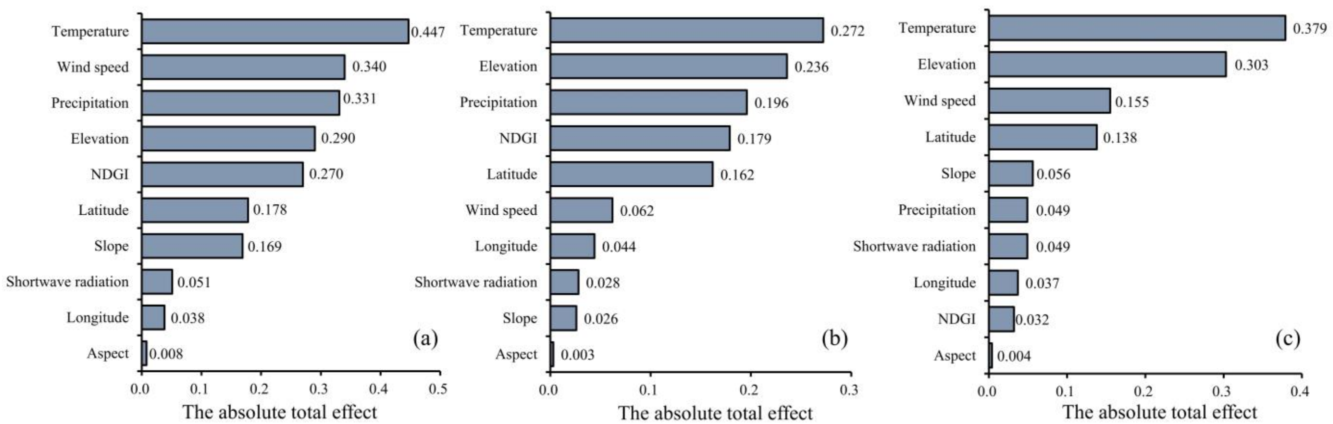

Figure 6: The absolute total effect of associated factors affecting SP ~~based on SEM.~~ of (a) SCD, (b) SOD, and (c) SED based on SEM.

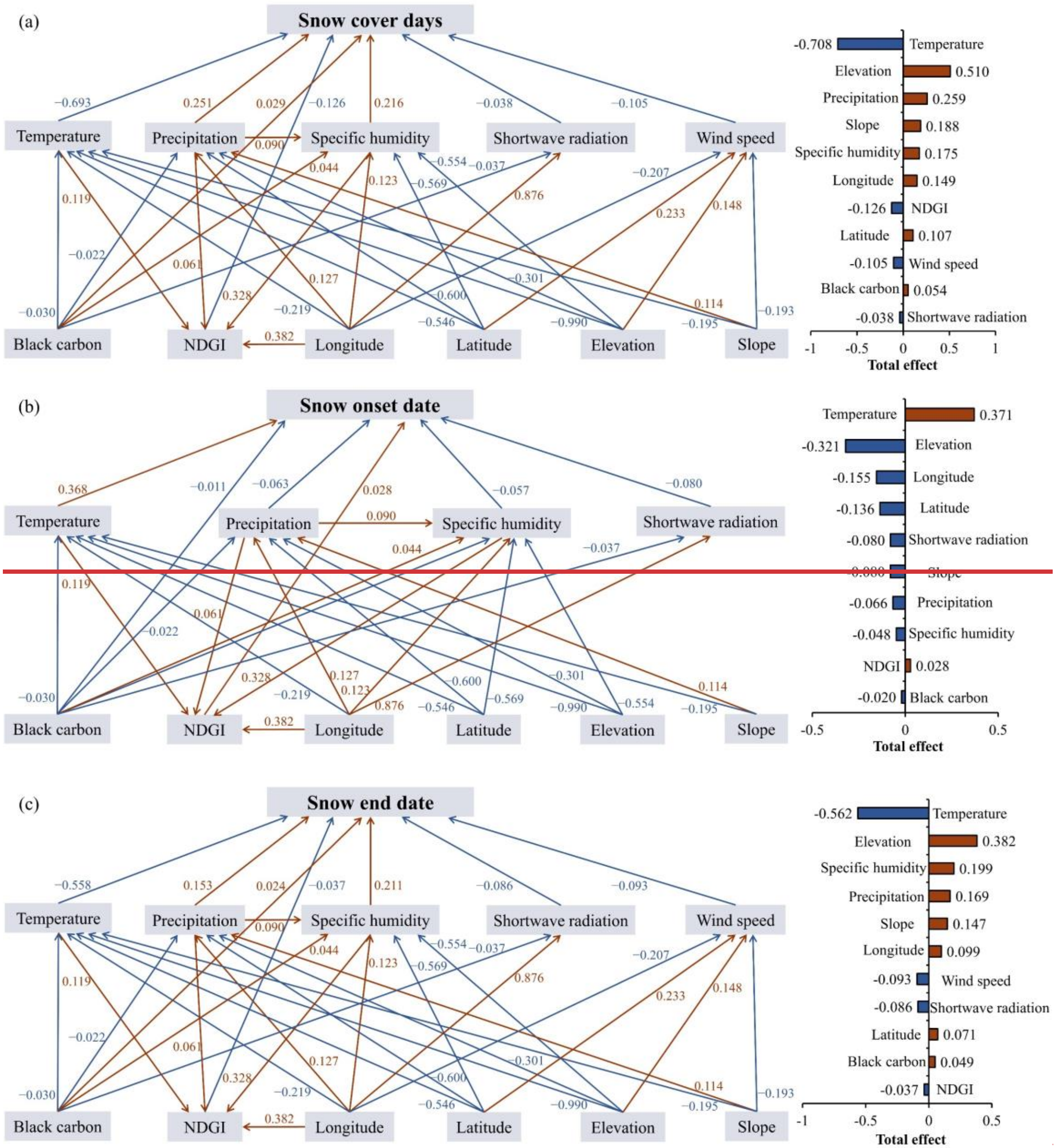
(a)
Snow cover days
Temperature
Precipitation
Specific humidity
Shortwave radiation
Wind speed
Black carbon
NDGI
Longitude
Latitude
Elevation
Slope
-0.708 Temperature
Elevation 0.510
Precipitation 0.259
Slope 0.188
Specific humidity 0.175
Longitude 0.149
-0.126 NDGI
Latitude 0.107
-0.105 Wind speed
Black carbon 0.054
-0.038 Shortwave radiation
Total effect
(b)
Snow onset date
Temperature
Precipitation
Specific humidity
Shortwave radiation
Black carbon
NDGI
Longitude
Latitude
Elevation
Slope
Temperature 0.371
-0.321 Elevation
-0.155 Longitude
-0.136 Latitude
-0.080 Shortwave radiation
Slope
-0.066 Precipitation
-0.048 Specific humidity
NDGI 0.028
-0.020 Black carbon
Total effect
(c)
Snow end date
Temperature
Precipitation
Specific humidity
Shortwave radiation
Wind speed
Black carbon
NDGI
Longitude
Latitude
Elevation
Slope
-0.562 Temperature
Elevation 0.382
Specific humidity 0.199
Precipitation 0.169
Slope 0.147
Longitude 0.099
-0.093 Wind speed
-0.086 Shortwave radiation
Latitude 0.071
Black carbon 0.049
-0.037 NDGI
Total effect

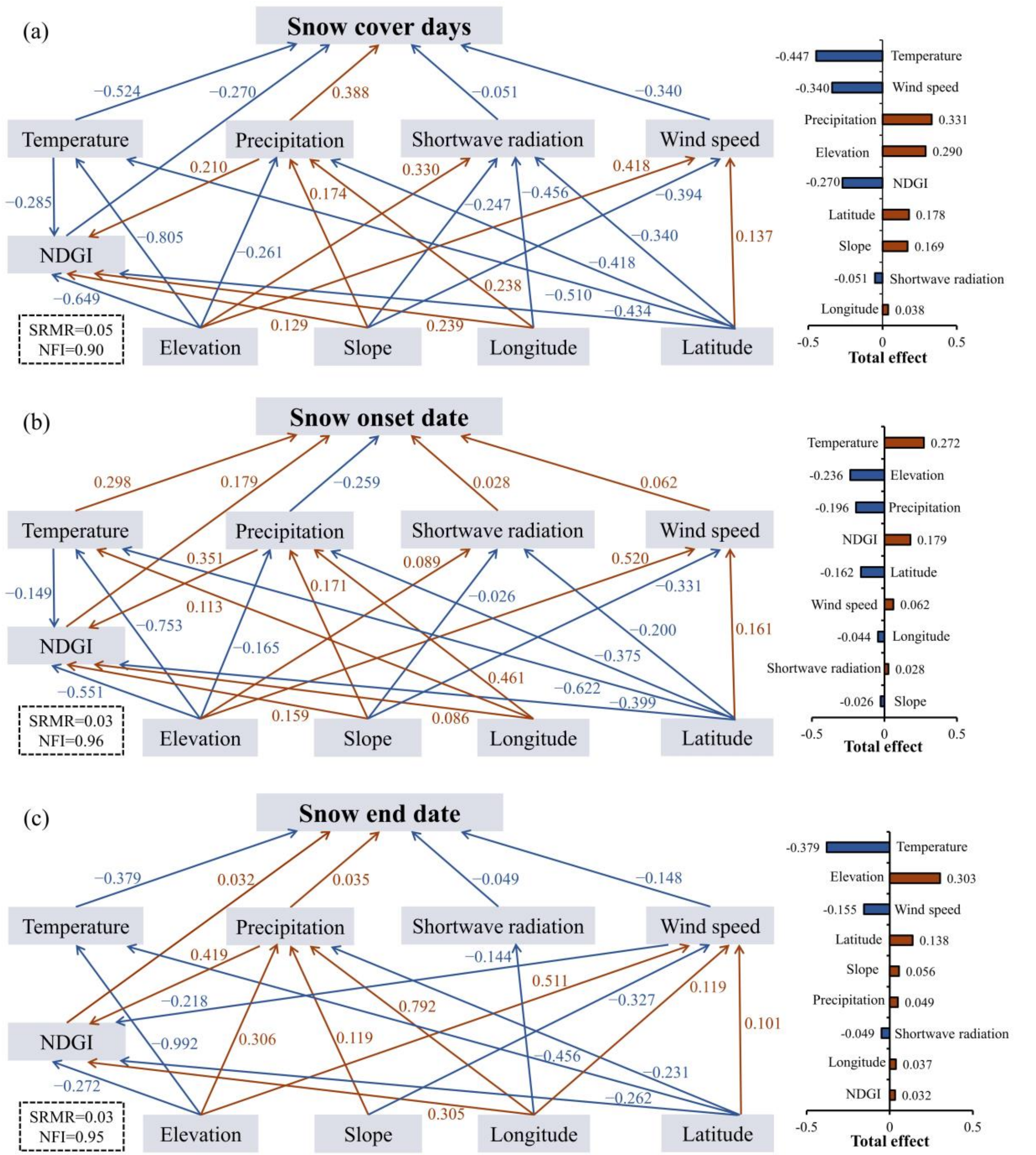

Figure 7: The ~~final~~ SEM of each SP parameter~~.~~ of (a) SCD, (b) SOD, and (c) SED. Note: the red line implies a positive effect, while the blue line denotes a negative effect. All path coefficients are statistically significant ($p < 0.05$).

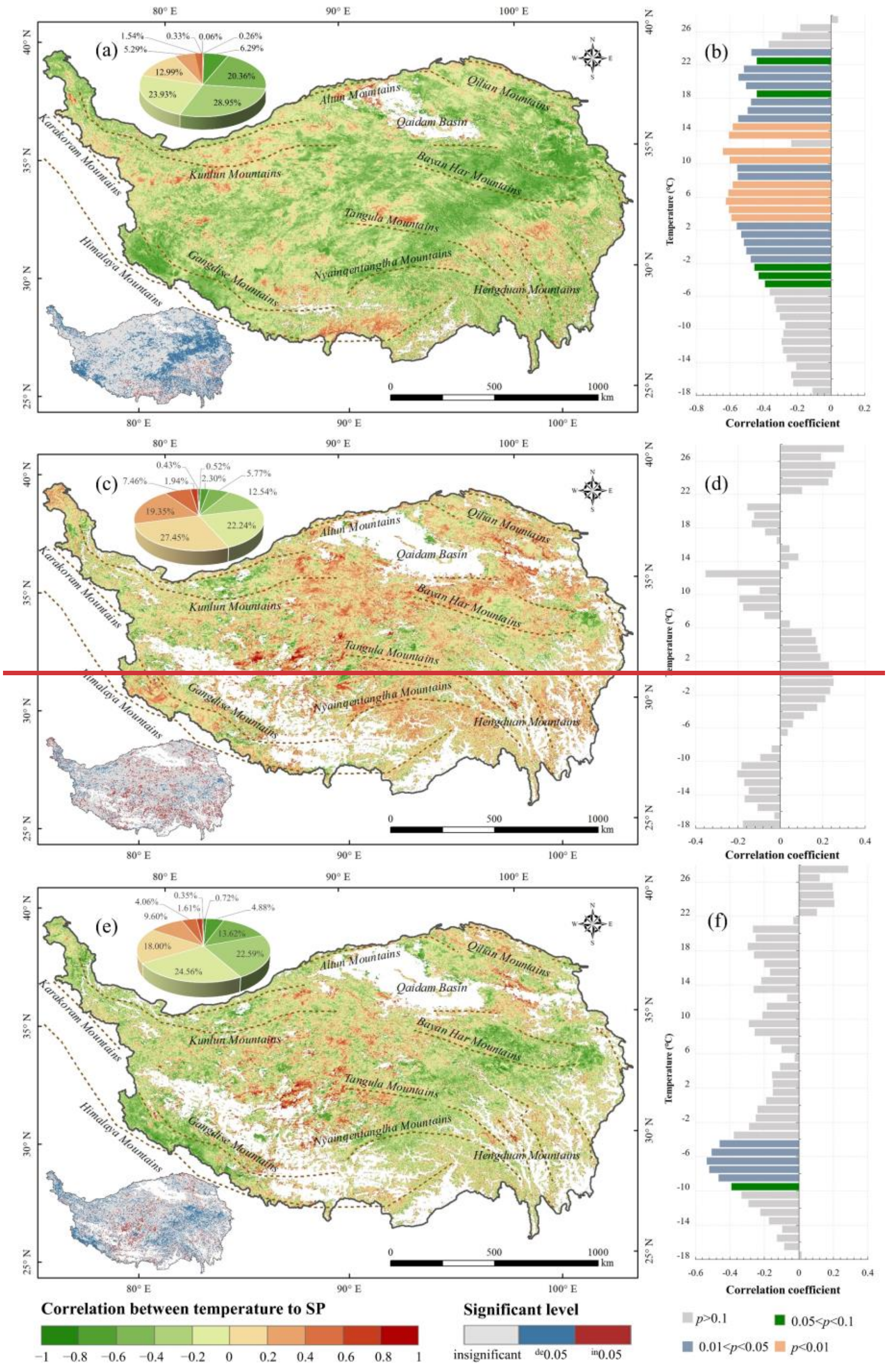
(a)
(b)
(c)
(d)
(e)
(f)
Altun Mountains
Qilian Mountains
Qaidam Basin
Karakoram Mountains
Kunlun Mountains
Bayan Har Mountains
Tangula Mountains
Himalaya Mountains
Gangdise Mountains
Nyainqentanglha Mountains
Hengduan Mountains
Temperature (°C)
Correlation coefficient
Correlation between temperature to SP
Significant level
insignificant
p>0.1
0.05<p<0.1
0.01<p<0.05
p<0.01

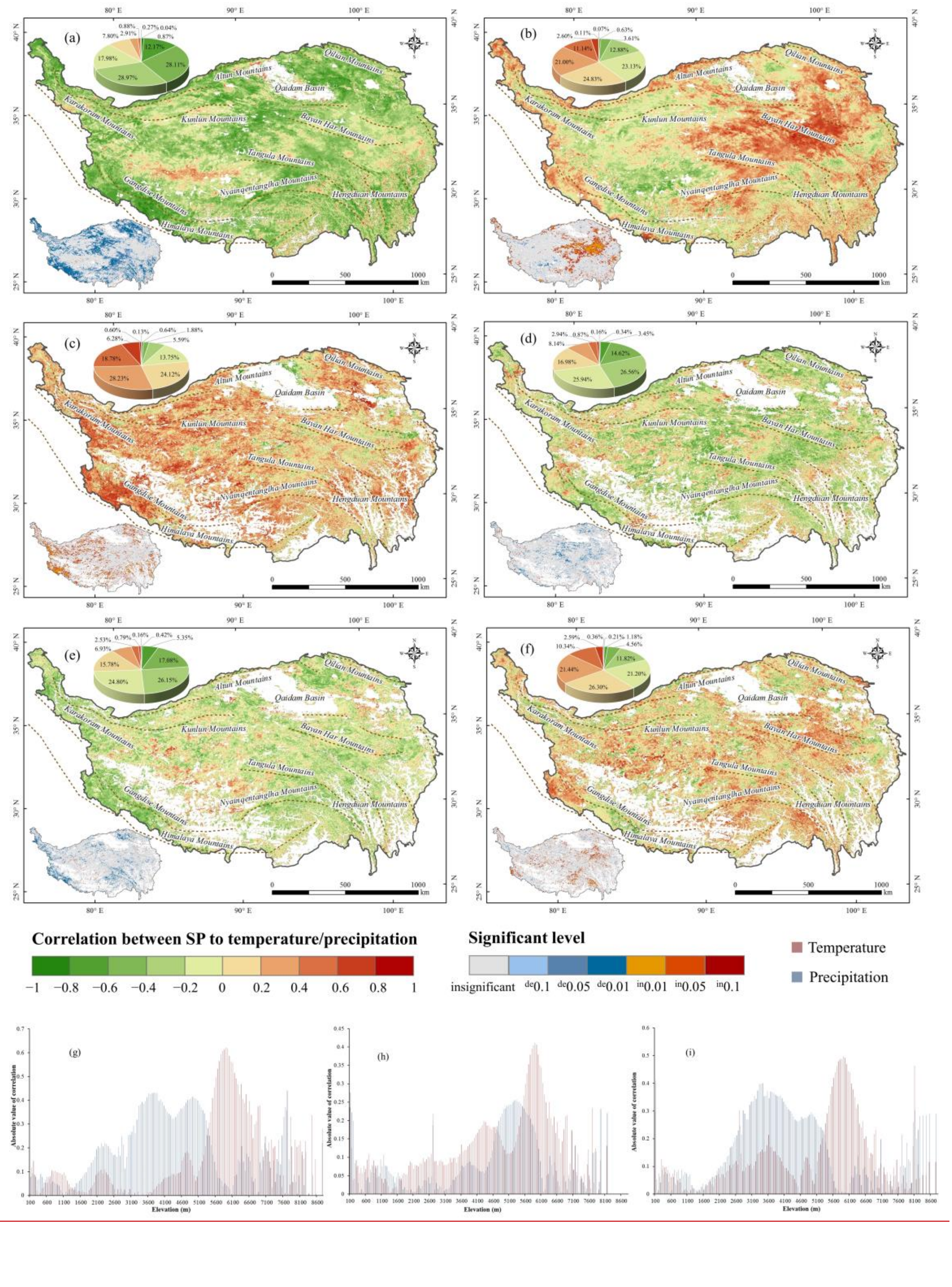

(a)
(b)
(c)
(d)
(e)
(f)
80° E
90° E
100° E
25° N
30° N
35° N
40° N
Qilian Mountains
Altun Mountains
Qaidam Basin
Kunlun Mountains
Bayan Har Mountains
Karakoram Mountains
Tangula Mountains
Nyainqentanglha Mountains
Hengduan Mountains
Gangdise Mountains
Himalaya Mountains
0
500
1000
km
Correlation between SP to temperature/precipitation
−1 −0.8 −0.6 −0.4 −0.2 0 0.2 0.4 0.6 0.8 1
Significant level
insignificant de0.1 de0.05 de0.01 in0.01 in0.05 in0.1
Temperature
Precipitation
(g)
(h)
(i)
Absolute value of correlation
Elevation (m)

Figure 8: Correlation between temperature and SP ~~at pixel level~~ of (a) SCD, (c) SOD, and (e) SED at pixel level; and ~~at different temperature gradients for (~~correlation between precipitation and SP of (b) SCD, (d) SOD, and (f) SED~~.~~

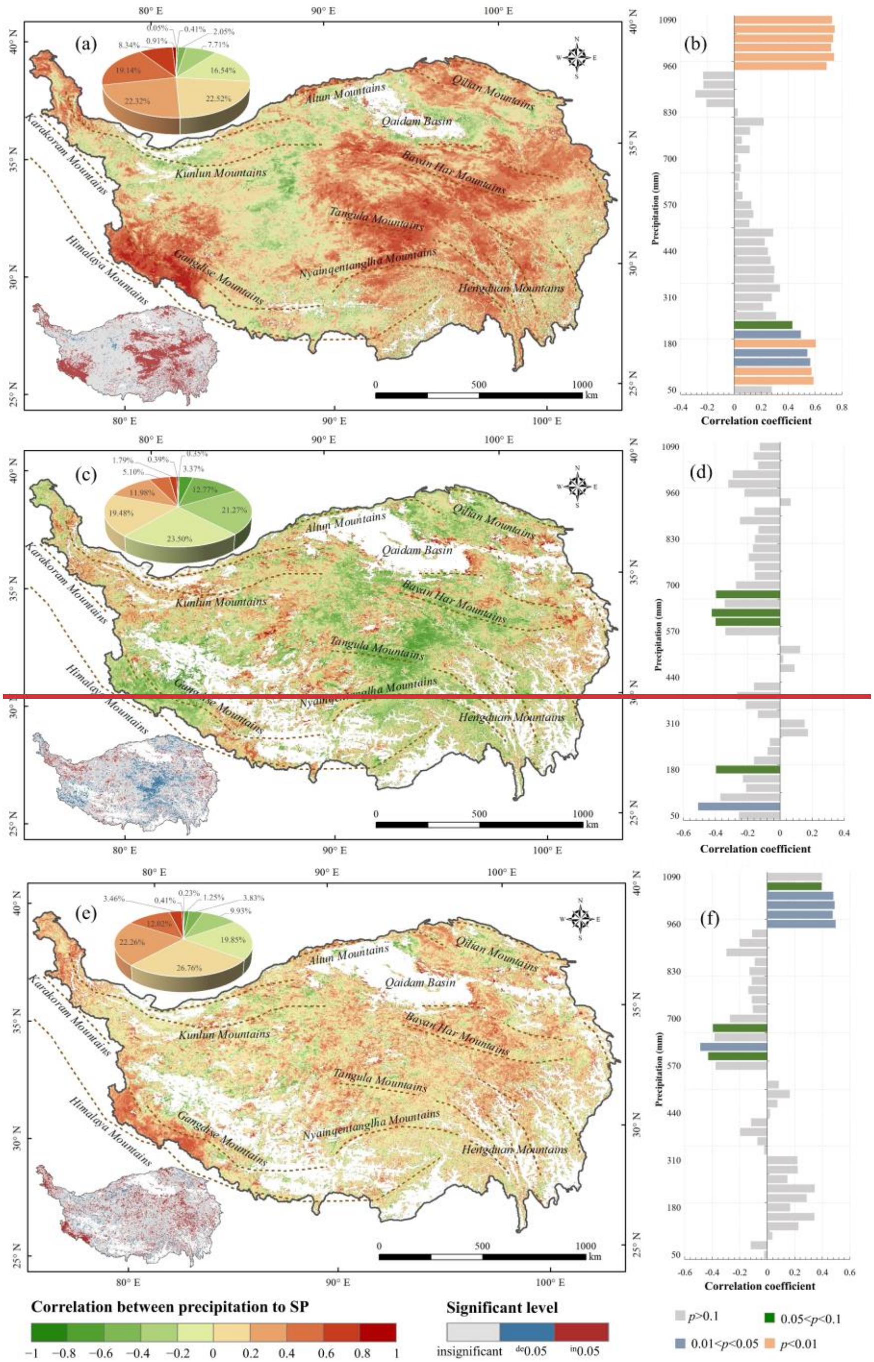

~~Figure 9: Correlation between precipitation and SP at pixel level of (a) SCD, (c) SOD,~~; and ~~(e) SED;~~ correlation coefficient between both temperature and ~~at different~~ precipitation ~~gradients for (b) SCD, (d) SOD, and (f) SED.~~

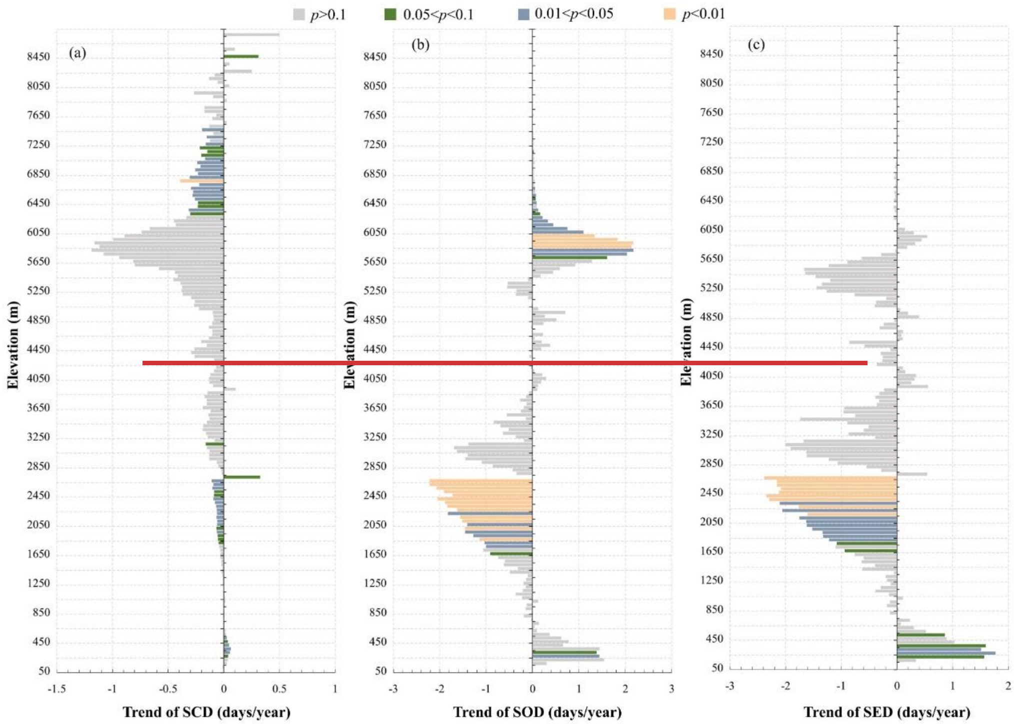

~~Figure 10: Interannual variation trend~~ and SP of ~~SP~~ (g) SCD, (h)SOD, and (i) SED under different elevation ~~gradients from 2002 to 2021. (a) SCD, (b) SOD, and (c) SED.~~ranges.

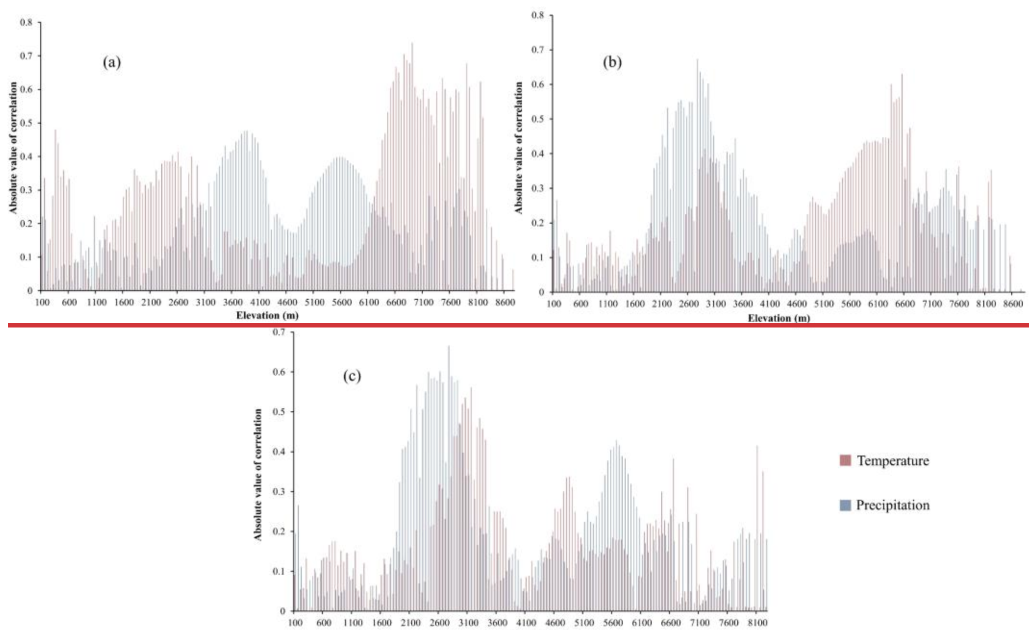

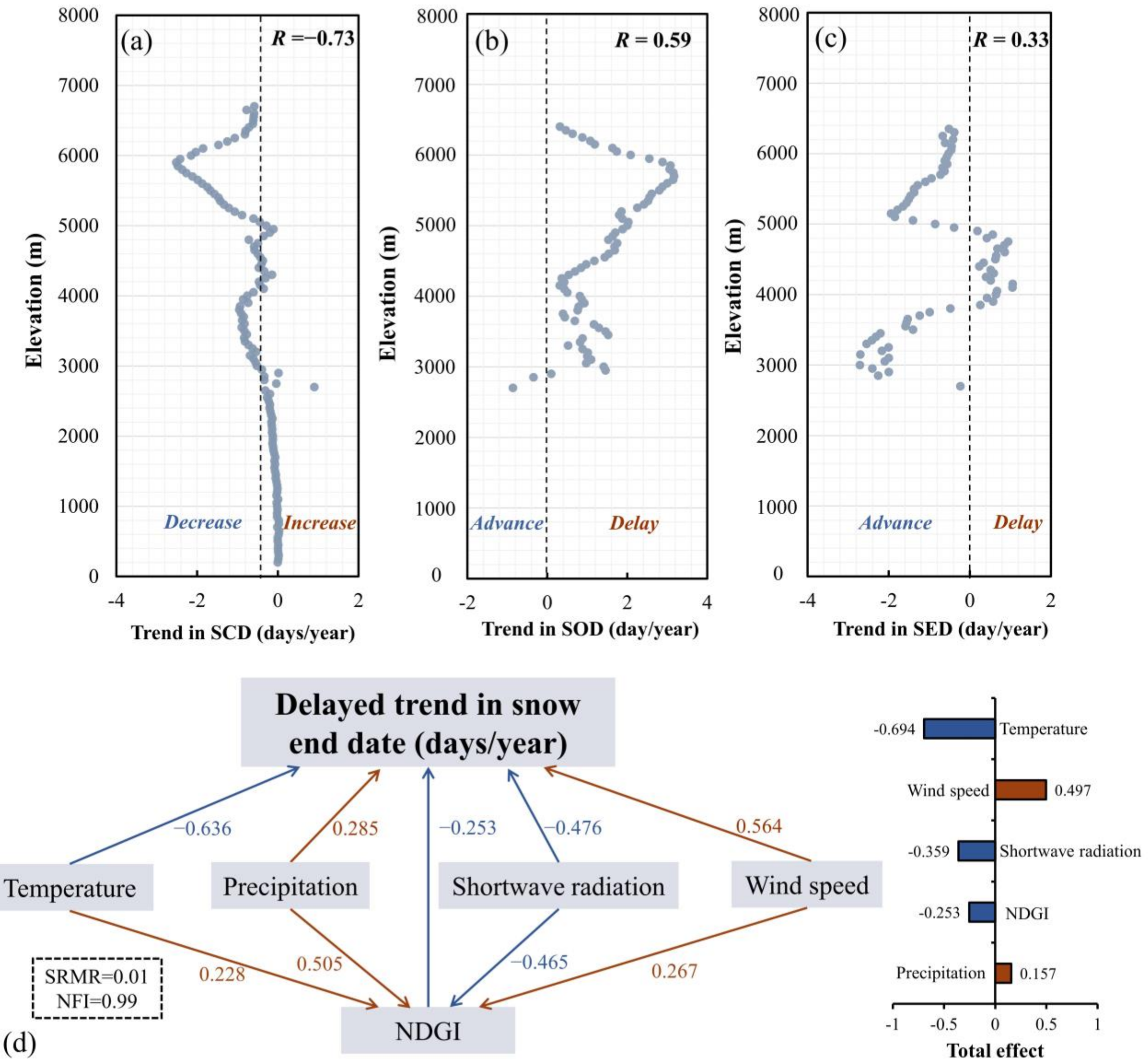

Figure ~~11: The correlation between~~9: Trends in SP of (a) SCD, (b) SOD, and ~~temperature/precipitation~~(c) SED under different elevation ~~gradients. (a) SCD, (b) SOD~~ranges on the TP from 2002 to 2022, and ~~(c) SED.~~

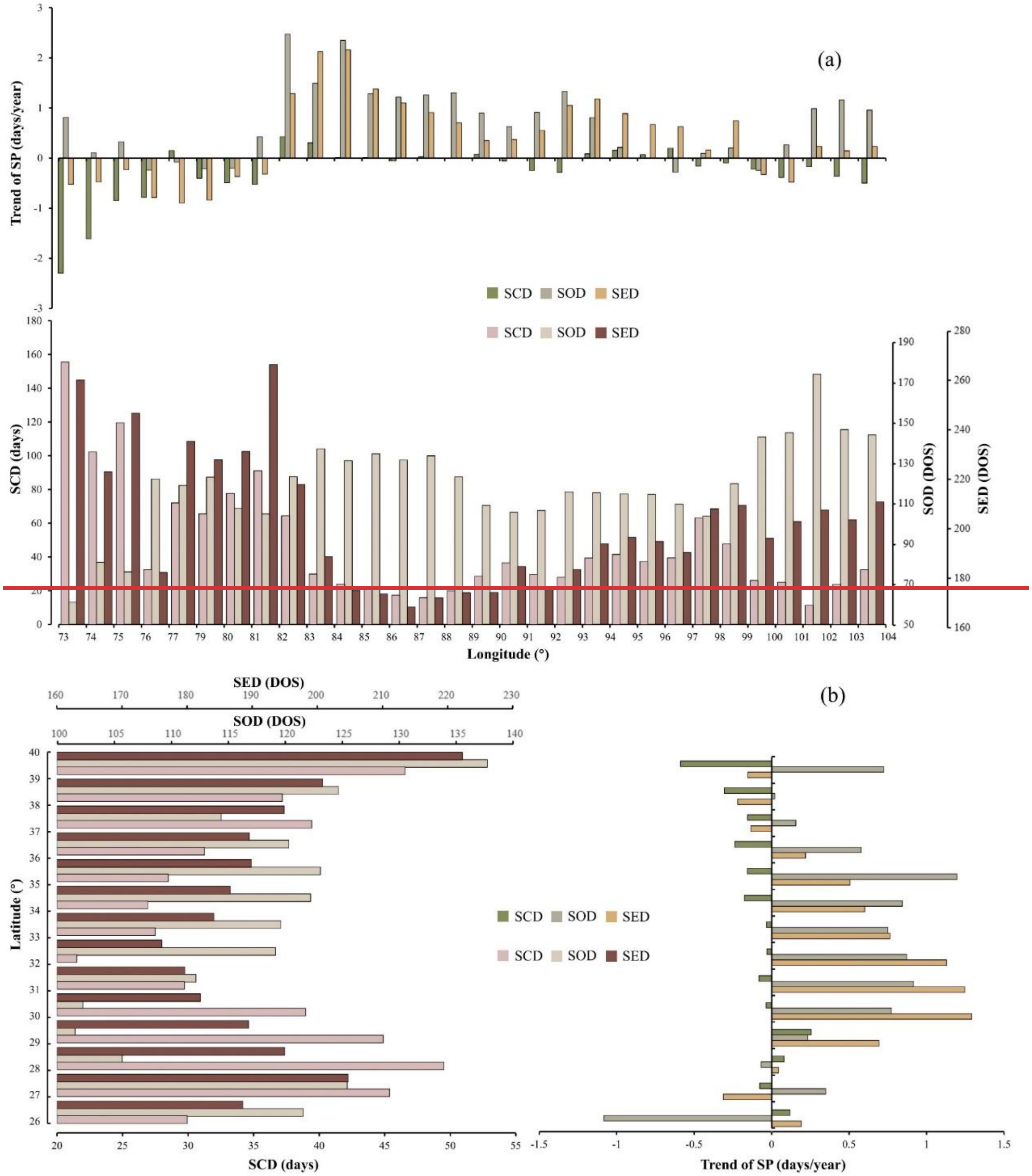

~~Figure 12: Multiyear averaged SP~~the SEM based on delayed trend in SED and ~~interannual variation trends associated to~~influencing factors (d).

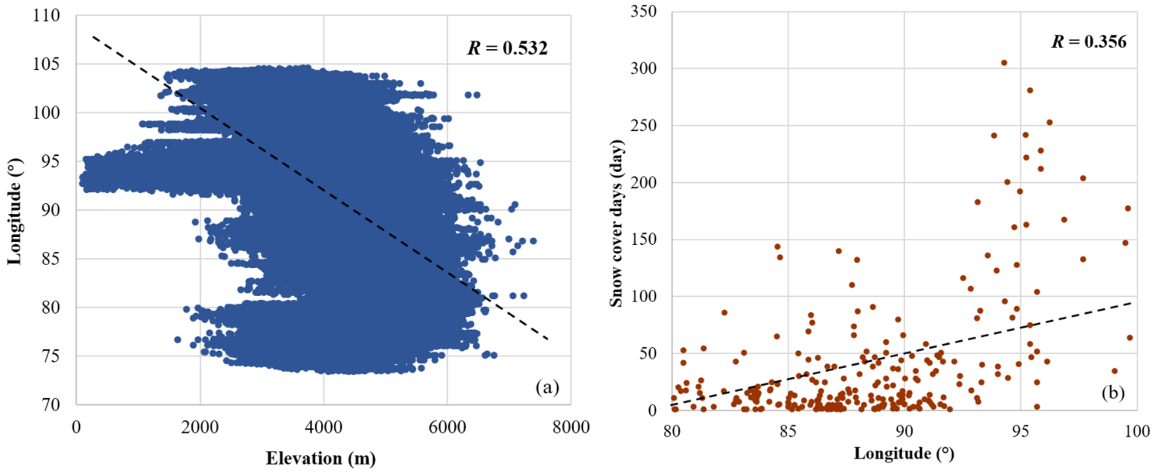

Figure 10: Scatter plot of (a) elvation and longitude~~ and~~, (b) ~~latitude. Note: no samples at~~ longitude ~~78°E–79°E.~~ and snow cover days (at a fixed elevation of 5000 m).